Alma Mater Studiorum - Università di Bologna

SCUOLA DI INGEGNERIA E ARCHITETTURA

Dipartimento di Ingegneria civile, chimica, ambientale e dei materiali

CORSO DI LAUREA IN CIVIL ENGINEERING

TESI DI LAUREA
in
STRUCTURAL STRENGTHENING AND REHABILITATION

SEISMIC VULNERABILITY OF THE ANCIENT ALBERGOTTI'S MANOR IN AREZZO, ITALY

CANDIDATO
Anna Chiara Faralli

RELATORE:
Chiar.mo Prof. Andrea Benedetti

Sessione II

Anno Accademico 2012/2013

Per onorare la tradizione…ai Senatori.

Audentes fortuna iuvat.
Virgilio, *Eneide,* X, 284

Index

Introduction 8

CHAPTER 1- Historical reconstruction and primary investigation.....10

1.1 Historical reconstruction of the case study 10

1.2 An overview of the structure 14

CHAPTER 2- Plan views and facades reconstruction.....23

2.1 Steps of the reconstruction 23

CHAPTER 3 -Stone masonry and its properties.....30

3.1 Introduction 30

3.2 Masonry and its properties 32

3.2.1 Characteristics of the elements of masonry 33

3.2.2 Mortar 34

3.3.3 Stone 35

CHAPTER 4- A non-linear static analysis: the Pushover Analysis 38

4.1 Introduction 38

4.2 Pushover analysis 39

4.2.1 Capacity curve 42

4.2.2 Linearization of the capacity curve 43

CHAPTER 5- Capacity Spectrum Method (C.S.M.) 45

5.1 C.S.M. description 45

5.2 Demand Spectra: elastic and inelastic 48

5.3 Fajfar's method according to the new seismic regulation 50

CHAPTER 6- Structural modeling and analysis.....54

6.1 Software and main assumptions 54

6.1.1 Mohr-Coulomb collapse criterion 55

6.2 Structural model 58

6.2.1 Materials modelling 58

6.2.2 2D Model 60

6.2.3 Load analysis and model of the actions 60

6.2.3.1 Gravity actions 61

6.2.3.2 Seismic forces 65
6.3 Design spectra 72

CHAPTER 7- Analysis of results and seismic assessment…….. 81
7.1 General approach 81
7.2 SLV Verification 81
7.3 SLD Verification 85

CHAPTER 8- Retrofit solution for slabs and vaults…….. 88
8.1 General considerations 88
8.2 Slabs retrofitting 89
8.3 Vaults retrofitting 92

Conclusions 96

Bibliography 98
Historical sources 98
Publications 99
Textbooks 99
Regulations 100
Manuals 100

Attachments 101
A.1 102
A.2 103
A.3 108
A.4 109
A.5 110

Introduction

This final dissertation aims at analysing an existing historical masonry building, which is, thus, investigated under a plurality of aspects.

First of all, a full historical study is provided in order to better clarify the construction path as well as understanding the high relevance of such heritage; then a detailed reconstruction of the plan views and facades is delivered thanks to a metrical evaluation on field and photographical methods.

Once all the components of the structure have been completely defined, a virtual representation is given by means of the finite element method using Straus7 software: in this way 2D views of the principal walls are created, allowing further studies.

Finally a pushover analysis is carried out for the two main directions aiming at determining the seismic capacity of the structure.

The very last section of the analysis is focused on possible retrofits for the construction: in particular, two different types of intervention are covered, explaining why they are considered a good choice for the case study.

Chapter 1

Historical reconstruction and primary investigation

1.1 Historical reconstruction of the case study

Dealing with an ancient structure, history represents the key point that makes us understand the whole development of the building in a proper way: for this reason a chronological description of the construction phases has been carried out by means of consultation of all kind of historical records.
This first part aims at showing the results of the reconstruction of the history of "Villa I Bossi", which is a medieval mansion property of Counts Albergotti and placed in Gragnone, a little village near the city of Arezzo (Tuscany).
The primary investigation was conducted throughout several readings from the personal hardcopy archive of the family, then the consultation of the city's historical and contemporary land register showed a *cultural property restriction* was set in 1998; hence the research moved to the city "Superintendence for Cultural Heritage" where documents testifying this event are collected. Finally the reference work done completed the investigation giving a conclusive view on the whole historical process the building has gone through.
The result of this first step is shown in the next paragraph; by the way its conciseness is basically due to the fact that the analysed mansion has been

always a property of the same family so that a poor documentation was provided since there was no interest in describing its state or structure (it would have been different if, for instance, the villa had been sold to the public authority or simply to someone out of the family since, in this case according to the usage of the period, a detailed description of the structure would have been provided).

The area, built up during the XVII-XIX centuries, includes an ancient small fortification dating back to the XIII-XIV centuries and already owned by the Albergottis placed as a defence of the Bagnoro and Arezzo's valley.
Enlarged time after time and turned into a mansion with a pertaining farm, the compound had been further subdivided and enlarged for estate's reasons since the mid-to-late of the XVIII century when part of the villa was handed to the Pandolfini family.
Partially visible from the courtyard dividing the two existing properties, the ruins of the medieval fortification and the keep (*mastio*) expose the very first *facies* of the building. Ruled by the Florentines in March 1384, the structure gradually lost its defensive purpose until the second half of the XVI century when it became "casa da padrone e da lavoratori", property of Nerozzo Albergotti.
At the end of 1500 the whole compound was inherited by Cav. Girolamo di Nerozzo, who left it to his sons Albizio and Cosimo in 1636; in particular thanks to the latter the very first arrangement of the villa and the chapel dedicated to S. Cristina was defined (1648). When Cosimo Albergotti (1619-1669) died, Senator Roberto Pandolfini and Cosimo's brother Albizio contended for his personal assets.
However we have to wait until 31th July 1745 to find in the land register the following note: " …Un tenimento di più pezzi di terra lavorativa, vignata, parte quesrciata e castagnata, sodo con parte arboreta e olivata, diviso per via che va a Roselleto, con casa da Padrone e Chiesa di staiora 54 (one staiora

is the area of land needed to seed a precise amount of wheat) posto nel Comune dei Bossi luogo detto Col di Gragnone e Sala confina: I) fiume di Col di Gragnone, II) via che divide il Comune di Bossi con quello di Pieve al Bagnoro, III) fossato che divide detti comuni e altri beni del medesimo Cosimo Albergotti e cav. Albizio e via che va al Roselleto.

Stima 320; … (list of other possesions)… sic ass il nome di Cosimo Albergotti già defunto e la presente posta incominciante in questo a carta 425 (Ancient land register of the city of Arezzo- Porta S. Spirito) si rinnove tutto in conto e faccia del colonnello Ferdinando del Sen. Camillo del Sen. Ruberto Pandolfini, erede mediante la persona del detto senator Ruberto suo nonno di detto Cosimo Albergotti e da esso nella persona di detto Sen. Camillo suo padre entrambi defunti ed oggi detto colonnello Ferdinando, come figlio, nipote ed erede rispettiavmente di detti suoi autori tutto con presenza ed istanza di Giovan Domenico Bonci agente del medesimo…".

Lacking of the majority of the manor-house, the Villa Albergotti was handed in 1672-1673 on brothers Alberico and Giovan Battista di Albizio; in that regard it is remarkable to mention the next description included in the land register: "… Un tenimento di terre lavorative, vitate, arborate, olivate e vignate con alcuni quercioli con casa da padrone e lavoratore di stajora 13 nel detto commune di Bossi, luogo detto Col di Gragnone fino a tutta la Grillandetta o Rio della Doccia, a levante e ponente: case di Cosimo Albergotti, tramontane: via della Casella o Roselleto; ponente: loro detti e detto Cosimo Albergotti, mezzogiorno: fossato della Doccia e beni di detto Cosimo stimato fiorini 52". (Land register of the city of Arezzo – Porta S. Lorentino ac. I23v).

It is interesting to notice that the number of *staiora* is reduced from 54 to 13 and that the area had been deprived of the church and it still bordered on Cosimo Albergotti's property even 4 years after his death.

During the second half of the XVIII century the Albergottis reached its political and economic apogee and the property, owned by Angelo Tommaso, underwent a series of extensions in order to become a sort of little palace

which actually could show the glory and pride of the family, just then titled as Marquise of Polino by the ancient family of Castelli.

Even Monsignor Agostino Albergotti, brother of the new marquise Angelo Tommaso, played a crucial role in the renovation of the building. Born in 1755, Agostino, who had always loved to take refuge in his villa in Gragnone, was appointed as bishop of Arezzo in 1802 and he was strongly engaged in reforming and founding religious orders as well as restoring churches and buildings owned by the Diocese: in particular he is recorded as the one who put through the Chapel of the Madonna del Conforto in the Arezzo's Cathedral and also the Church of Santa Caterina, next to the Albergotti's palace in the city centre.

The enlargement works carried on at least until the first decade of the 1800s, when the Marquise Giuseppe acquired the whole property, son of Angelo Tommaso. At that period the land register annotates: " … un palazzo ad uso di villa di n°43 stanze da cima a fondo, con orto e i suoi annessi con Oratorio modernamente costruito cui confina: 1° Sig.ra Contessa Cassandra Pandolfini con Villa; 2° e 3° beni infrascritti annesi a detta villa; 4° strada. Stimato: fiorini 190 che non si tirano fuori poichè atteso servire proprio uso…" (Transfer of registration 1807-Book II ac.748).

1.2 An overview of the structure

Villa Albergotti-Pandolfini is located in Gragnone, a small village 6 km far from the city of Arezzo (Tuscany).

Picture 1. Building location

Picture 2. Aerial view

The main building is a three-storey masonry structure made up by 4 principal bodies all connected to a large inner courtyard. The main plan dimensions are equal to 20,30 x 24,84 m, while the interstorey heights are really different due to the misalignment of the majority of slabs (3,50 m on average with maximum height of 5,10 m and minimum of 2,50 m).

Picture 3. Aerial view 2

Well-preserved and recently refurbished, Villa Albergotti shows a façade characterised by rectangular aligned windows and its left side is linked to Villa Pandolfini characterized by *bugnato* gate, which, once, was connected to the front park by means of a little stone bridge. Absorbed within the villa, the mighty tower of the ancient *mastio* stands out against the whole compound and it is placed side by side with a segmental arched turret.

Picture 4. Main facade

Next to the main building we find the chapel, bordered by two angular pilasters with a portal and an over standing window. The inside, composed by only one big rectangular hall, displays XIX century *trompe-l'oil* trimming over doors, recesses, confessionals and windows. The imitation marble altar shows a painted trabeation framing a XVII-XVIII century canvas that depict the Immaculate Conception.

Assigned to farm purposes, the ground floor reveals plenty of statements of the medieval fortification with plugged portals and *a ferro di vanga* coats of arms of XIII-XVI century: all these early elements are well mixed with more modern ones, for instance the wood truss on the ceiling as a substitute of the ancient vaults whose marks are still visible on the stone walls. From the ground floor a stone stair, garnished with the Albergotti's emblem, leads to the upper floors.

Enriched by wide boardrooms, the first floor is the result of the improvements conducted by the brothers Angelo Tommaso and Agostino Albergotti; the halls, full of XIX century frames and trimming, exhibit XVIII-XIX century fireplaces made of stone or imitation marble.

Given exclusively to bedrooms, the second floor is, on the other hand, composed only by alcove and *boudoirs* together with servants' settings.

The last part to be mentioned is the attic and the turret, which gives us a complete view of the park.

The most likely kind of slab is made of two orders timber beams according to the Tuscany way as shown in pictures 5, 6 and 7: all of them have been taken at ground floor where this element is prevailing; in addiction vaults are even widely used (see pictures 8 and 9), while few false ceilings are present.

Picture 5. Two orders timber beam slab 1

Picture 6. Two orders timber beam slab 2

Picture 7. Two orders timber beam slab 3

Picture 8. Example of little vaults 1

Picture 9. Example of little vaults 2

Finally the study of the roofing completes the preliminary investigation of the building; in this case the roof is made up by different elements connected one to the other as shown in pictures 10 and 11.

Picture 10. First floor roof connections

Picture 11. Second floor roof connections

If we look at the relative internal connections, we find timber trusses, which belong to a more recent refurbish. Pictures 12, 13 and 14 provide examples.

Picture 12. Inner connections of first floor roof

Picture 13. Detail of an Inner connection of first floor roof

Picture 14. Particular 2 of an Inner connection of first floor roof

Chapter 2

Plan views and facades reconstruction

2.1 Steps of the reconstruction

The next step is the reconstruction of the external facades, which will be used during the pushover analysis in order to simulate the performance of the main walls. Given the lack of general information on the structure, it was necessary to collect any useful pieces of news; furthermore, since no design blueprints were available, an accurate metrical survey was done in order to detect all the geometrical aspects related to the overall building as well as to the single components.: in particular, such work was even aimed at describing the changes the structure has undergone during its life.
In order to do so a direct photographical method is selected; the chosen approach, even though it is a simplifying one, is operatively functional to streamline the whole process giving a quick result. The main steps of this procedure are:

- *Photographical and metrical evaluation on field:* by means of measuring stake and laser distanziometer a preliminary metrical evaluation is done for each floor; in addiction a photographical survey is conducted in order to take note of any particular structural elements or any substantial peculiarity. At this stage photos of all the facades are taken: the technique is simply based on trying to take pictures from the most far point such that the whole façade can be seen. Obviously a check of the main measures is needed in order to reduce the uncertainty due to the imperfection of the picture itself.

- *Definition and updating of plan views*: they are useful mainly to get a correspondence between the façade representation and the perimeter measurements; in fact, at this stage, the plan view gives a complete visualization of the structure as well as a broad orientation of the structure in space. At this stage, software AutoCAD has been used in order to draw the main three plan views displayed in picture 16, 17 and 18: notice that some part of the initial reconstruction (picture 15) are not considered for sake of simplicity and, basically, because they can be viewed as additional components that are not relevant for the following analysis.

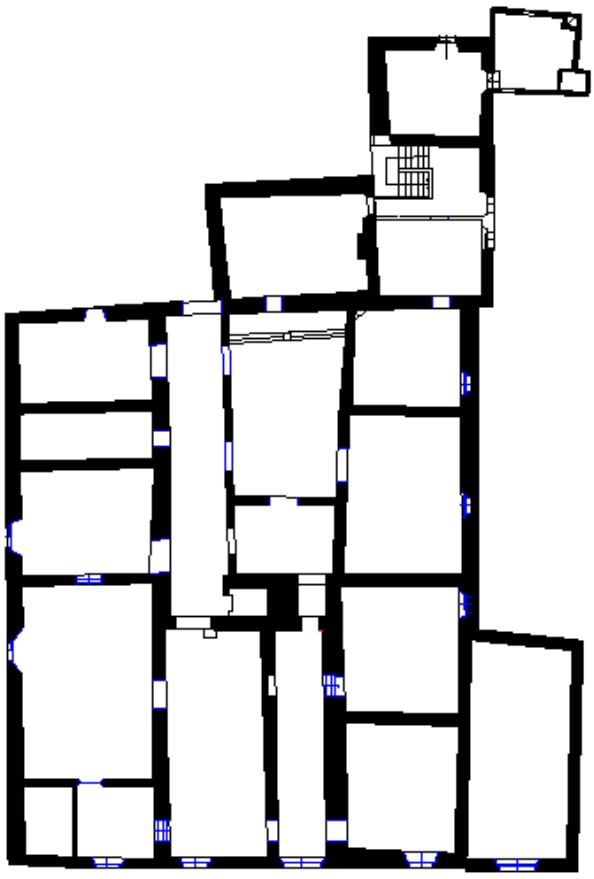

Picture 15. Plan view reconstruction

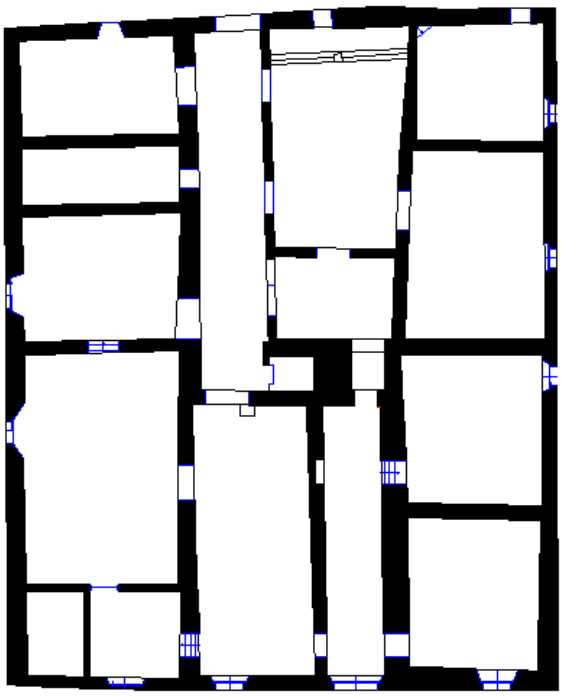

Picture 16. Ground floor plan view

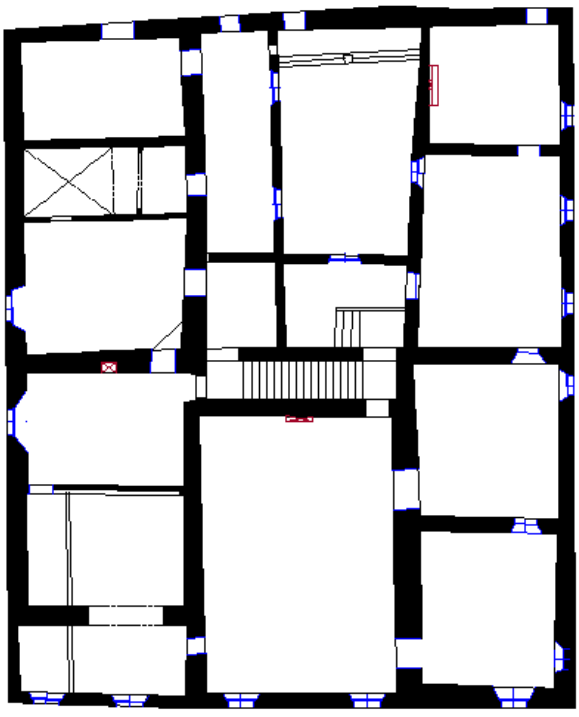

Picture 17. Raised ground floor plan view

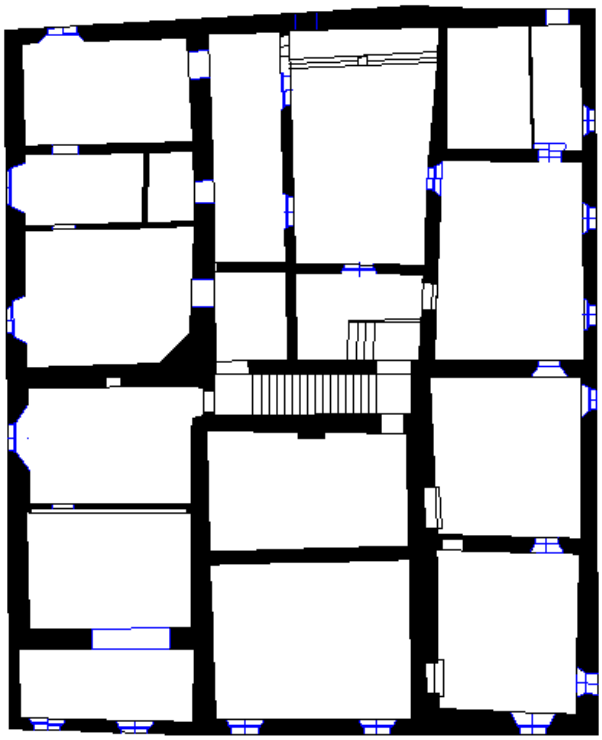

Picture 18. First floor plan view

- *Reconstruction of facades*: given pictures of all the main facades and the heights of the structure, a frontal reconstruction of the building is provided; this will be the initial point for the virtual modelling. Pictures 19, 20 and 21 provide examples concerning the front and right lateral walls: in particular picture 19 shows the superposition of plan view and photographical data, while pictures 20 and 21 represent the real reconstruction of the facades. This kind of work has been done both for internal and external walls. For a clearer display of them see the attached blueprint 1.

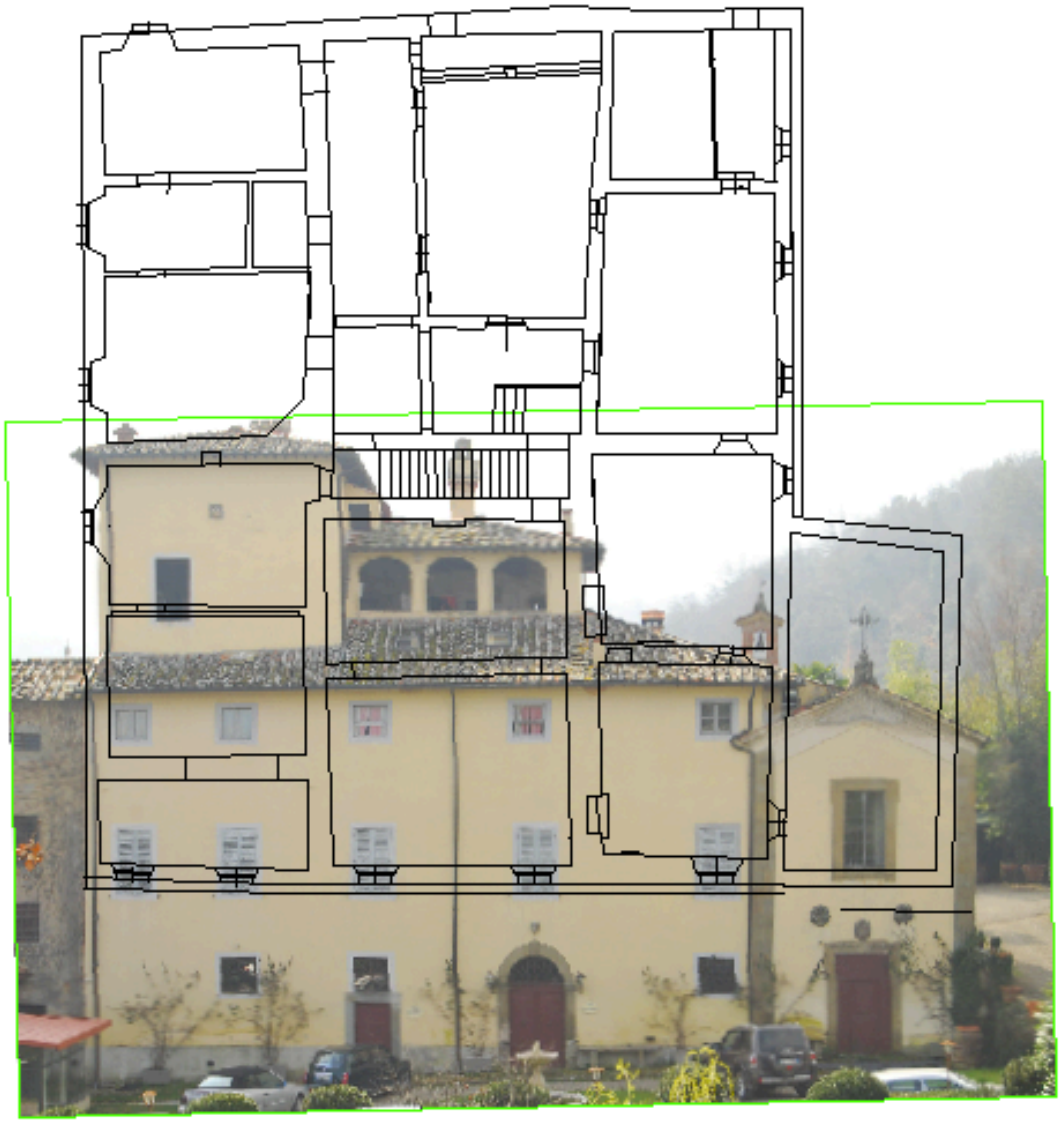

Picture 19. Use of photograph to orientate and define the façade reconstruction

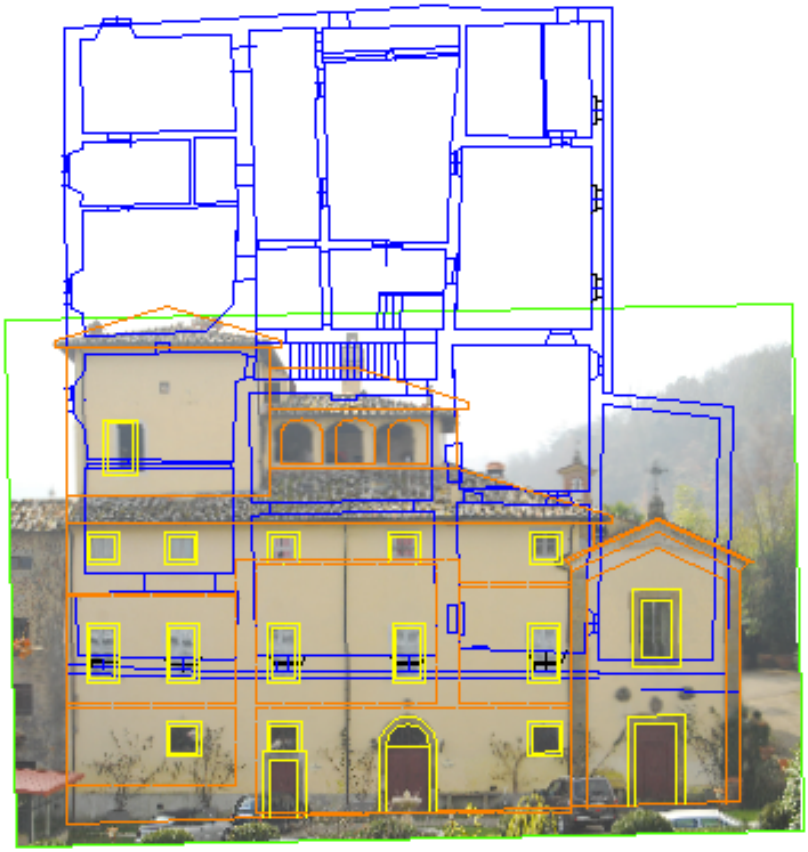

Picture 20. Main façade reconstruction

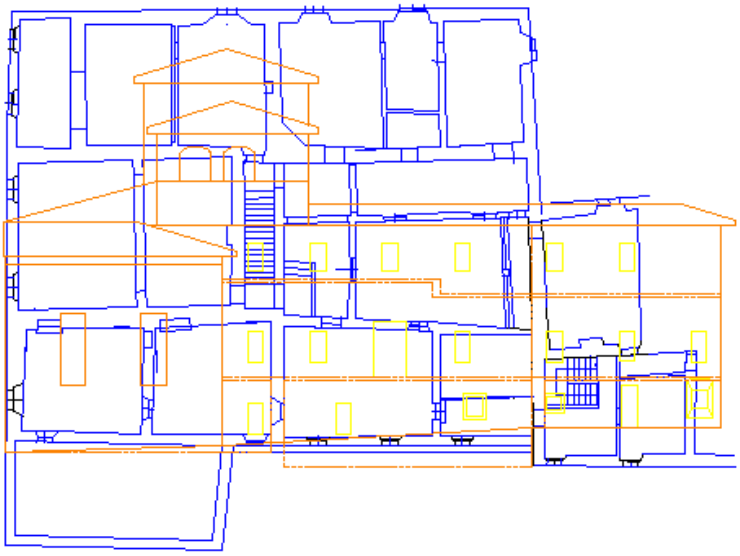

Picture 21. Lateral façade reconstruction

Picture 22. Final front façade

Moreover, as we can see from picture 22, the internal heights have been even reconstructed for each wall, showing a quite irregular inner arrangement as well as plenty of gaps: this will lead to the need of creating a more detailed virtual representation in order to take into account the real disposition of the elements.

Eventually, a check of thicknesses is done pointing out that walls are characterized by a wide range of widths (30-65 cm): for this reason we set their value to an average one equal to 50 cm.

Chapter 3

Stone masonry and its properties

3.1 Introduction

The behaviour of masonry buildings within a seismic context is one of the most important and interesting current matters given the wide spread of historical masonry structures in our country: in fact, the huge Italian artistic heritage is still mostly composed by such constructions and it is really essential to preserve them to make them last as much as possible.

Unfortunately, the high level of seismicity of Italy has repeatedly represented a hard curse to bear and, now more than ever, we need to deeply investigate and forecast any possible consequence of this kind of action.

According to studies conducted since '60s, we know that, when talking about masonry structures, we actually refer to a wide range of different buildings so that we should expect different kinds of seismic response; besides, it has already been shown that this variety is linked to technological aspects generally depending on the site category, historical period and usage.

Moreover, the type of used materials seems to be fundamental in order to better describe the real behaviour of structures, taking into account all the possible nuances that different strengths could give to different edifices.

In fact, the seismic performance strongly depends on the quality of the structure itself besides the kind of seismic action, so that it is necessary to carefully investigate the structural type as well as design process and detail of structural elements.

For instance, huge and critical seismic events, such as the 1978's in Friuli Venezia Giulia or the 1997's in Umbria or the 2002's in Molise, were the key point to actively start a deeper investigation on the main causes of such effects; in particular, the analysis of damaged masonry buildings and their actual capacities pointed out that the majority of harms were connected to structures whose construction lacked of effective knowledge or accuracy. As far as this matter is concerned, the main reasons could be:

- wrong structural idea
- non accurate design project
- poor material quality
- mistakes during the execution phase
- lack of maintenance
- changes of the building, leading to a static scheme which is different from the initial one

On the other side, masonry has its own advantages:

- quick and easy execution with respect to reinforced concrete or steel structures
- great ability to adapt to different environments, mostly required within historical city centres
- high durability
- very good performance for fire resistance, acoustic isolation and climate changes
- cheaper than reinforced concrete and steel

Unfortunately, there are even some disadvantages such as:

- smaller compressive strength than concrete's
- brittleness
- poor ductility
- strength reduction under cyclic loads (such as seismic action)

However, the previous negative aspects could be at least mitigate throughout a careful design as well as a correct execution, reaching a state where masonry structure can be considered safe even in highly seismic sites.

3.2 Masonry and its properties

Masonry is the very first composite material used for constructions: in fact, it is made of brick or stone and mortar and it is characterized by global properties, which are the result of the combination of its components'. Moreover, because of such an internal structure, masonry is nothing but an anisotropic material with prevailing sliding directions: for this reason, it is important to carefully estimate the consistency of all components.

First of all, the geometry and the disposition of the stones represent the greatest parameter in order to assess whether the quality is good or not: for instance, if the stones' dimensions are such that they occupy a big part of the thickness, we can immediately assume a satisfactory quality.

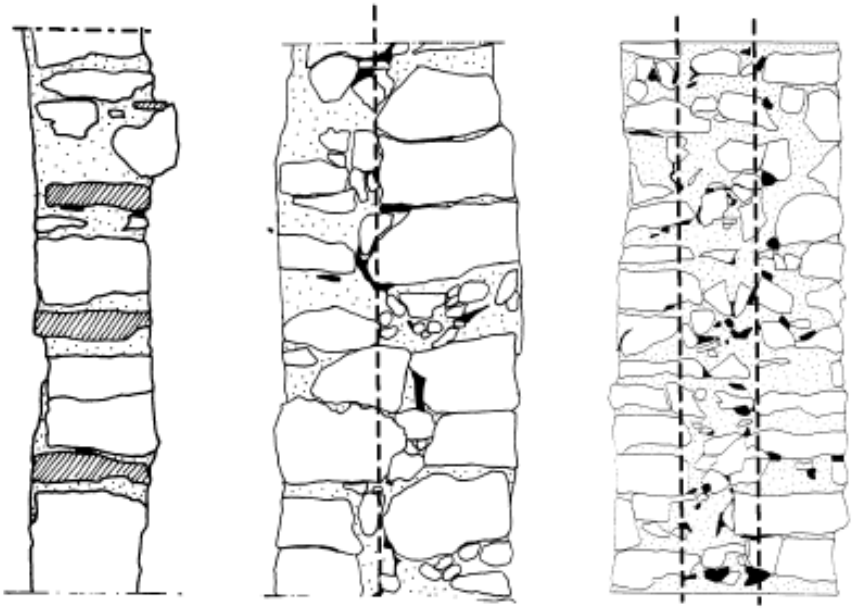

Picture 23. Different kind of transversal sections

According to what has been previously said, one of the most dangerous pities of a masonry wall is the lack of a transversal monolithic structure: this generally happens when the wall is made of little pebbles (see the right image in picture 23) or it is filled by disorganised elements between two external organised facades. Eventually, this aspect leads to an increase in wall's brittleness when it is subjected to external forces orthogonal to the wall's plane.

3.2.1 Characteristics of the elements of masonry

When talking about masonry we generally refer to a material made by resistant elements characterised by different kind of shape and connected or not in different ways.

Basically, these resistant elements can be made of:

- *stone*
- *brick*
- *concrete*

Moreover, the most common shape currently used is parallelepiped, while, if present, the connection is made of *mortar*.

3.2.2 Mortar

Mortar is mixture of water, sand and a bonding material; in particular, the latter is the one that states the kind of mortar: the most common are cement, hydraulic lime, hydrate lime and pozzolan. Moreover, additives can be included in order to get better performances such as pliability and waterproofing.

As far as the Italian regulations are concerned, we can have different classes for mortar according to their mean compressive strength f_m:

- M1 with $f_m \geq 12$ N/mm^2
- M2 with $f_m \geq 8$ N/mm^2
- M3 with $f_m \geq 5$ N/mm^2
- M4 with $f_m \geq 2{,}5$ N/mm^2

For each class the relative composition as well as the volumetric proportions of sand and binder.

When dealing with massive structures, the hardening of mortar is not a homogeneous process due to the problem of water evaporation in the deepest parts: such situation causes a strength reduction because of the creation of coactive states within the mortar. In this case, as the constructors of the past knew very well, it is necessary to leave each layer exposed to air to allow its full grip.

Finally, we should pay attention to the behaviour of the mortar in the joints since, due to environmental attacks, these zones are the most vulnerable with consequent reduction of the masonry's thickness.

3.3.3 Stone

Stone masonry was widely used in the past thanks to the low cost of work; it can be generally subdivided in:

- *Squared stone masonry*: characterised by great resistance, it is made of adjusted units linked by metallic bolts
- *Masonry with squared stone cover*: externally made of squared stone, while lower quality materials were used for the inner part
- *"Faccia vista" masonry*: internally made of bricks or concrete, while externally made of irregular stones
- *Tuff stone covered masonry*: cheap and easy to construct, it is generally used for small buildings or for overheads
- *Ordinary stone masonry*: it is carried out without any particular care from an aesthetic point of view; generally made of irregular units, which will be covered by plaster.
- *Mixed masonry*: bricks are used to fill the voids between stones.

However, according to NTC 2008 (Par. 7.8.1.2), non-squared stone masonry can be used only in sites belonging to zone 4, which is the one with the lowest seismic risk.

As far as the case study is concerned, investigations on field revealed that the most likely kind of masonry is the mixed type: as we can see in picture 24, stones are not squared, actually characterised by a very irregular texture.

Picture 24. Example of mixed masonry

On the other hand, brick elements are poor in number and basically placed in concentrate areas (around windows) or just represent the presence of previous openings that are now closed.

Picture 25. Example of ordinary masonry

Furthermore, we can even find ordinary stone masonry: picture 25 shows the adjustment of differently shaped stones spaced out by very thin mortar layers.

Chapter 4

A non-linear static analysis: the Pushover analysis

4.1 Introduction

The forecast of the seismic response of a structure requires some tools for a dynamic non linear analysis, which, on its side, means the integration of equations of motion of a MDOF (multi degrees of freedom) system; such a procedure seems too expensive and complex so that a different approach has been introduced: namely, a non linear *static* analysis.
This kind of method has two main advantages: being a static analysis, it is simple and really straightforward; moreover, it gives realistic and reliable results.

As far as its principles are concerned, there are two key points that characterise this process:

- Definition of a force-displacement relation, given by the so-called *pushover analysis*: the *capacity curve*
- Assessment of the maximum displacement of the structure after a seismic event defined by means of an elastic response spectrum: the *functioning point.*

4.2 Pushover analysis

The pushover analysis allows expressing the behaviour of the structure by means of a monodimensional relationship: this is nothing but a transformation of the initial MDOF system into an equivalent SDOF (single degree of freedom).
The general scheme of this approach can be defined as follows:

1. Demand: definition of response spectrum which is compatible to the local seismic activity
2. Capacity: creation of a MDOF model, thus performing the real pushover analysis
3. Response: generation of the equivalent SDOF system and relative reaction; eventually this system have to be reconverted into a MDOF
4. Verification: definition of the global performance of the structure.

The pushover analysis, in this sense, works as a non linear static procedure: in practice, we literally push the structure to its collapse point or until a control deformation parameter is reached. Moreover, such a "pushing action" is defined by incrementally applying (in a monotonic way) a design forces or displacements profile (*method of incremental-iterative solution of the static equilibrium equations*).

As an example, let's take a SDOF system (picture 26) idealized as a concentrate mass m supported by a massless element with k as lateral stiffness and linked to a damping element (no mass and no stiffness). In this case, the deformed shape is defined by only one parameter, which can be, for instance, the mass displacement with respect to the ground (D_t).

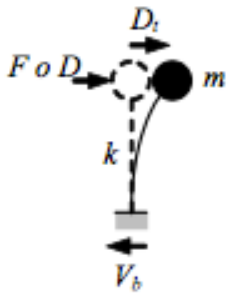

Picture 26. Schematization of a SDOF system

In such simple situations, the pushover analysis requires the application of a displacement D or force F system to the mass, gradually increasing their moduli in the direction of the only degree of freedom available. A mathematical representation can be:

$$D = \alpha d \quad (4.1)$$

$$F = \beta f \quad (4.2)$$

So, once d or f values have been arbitrarily set, the multipliers α or β are increased until we have a complete view of the response domain.
Moreover, the behaviour of the structure is defined throughout a force-displacement relationship where the force is equal to the base shear force V_b and the displacement is equal to mass's one D_t.

Moving to a MDOF system, a horizontal forces or displacements profile is applied at each floor (picture 27) and we need to select only one force and displacement parameter, whose choice is not univocal; generally base shear force and displacement of the centre of mass of the highest floor are taken.

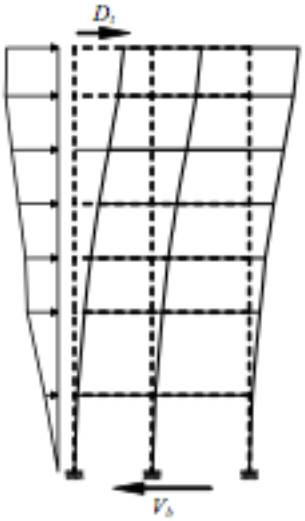

Picture 27. Scheme of a MDOF system

In this case, we set a displacement of forces profile as follows:

$$\vec{D} = \alpha\vec{d} = (D_1\, D_2 \ldots D_f \ldots D_n)^T \quad (4.3)$$

$$\vec{F} = \beta\vec{f} = (F_1\, F_2 \ldots F_f \ldots F_n)^T \quad (4.4)$$

where $\vec{d} = (d_1\, d_2 \ldots d_f \ldots d_n)^T$ *and* $\vec{f} = (f_1\, f_2 \ldots f_f \ldots f_n)^T$, while $D_i = \alpha d_i$ is the displacement at the ith floor and $F_i = \beta f_i$ is the force at the ith floor.

However, there are some doubts about which parameter choose as a reference between force and displacement: generally, the force approach is advised because of its simplicity of being implemented.

4.2.1 Capacity curve

The capacity curve represents the structure's ability to resist a certain seismic action; it can be displayed on a Cartesian plane where the x axis stands for displacement of the upper floor's centre of mass, while the y axis stands for the increasing base shear force.

For a SDOF system, the trend of the capacity curve depends on the stiffness k or on the flexibility k^{-1} of the structure itself, characteristics that depend, in turn, on geometrical and mechanical properties of the system:

$$F = k(D) \quad \text{oppure} \quad V_b = k(D_t) \tag{4.5}$$

$$D = k^{-1}(F) \quad \text{oppure} \quad D_t = k^{-1}(V_b) \tag{4.6}$$

Picture 28 shows three typical capacity curves where three main post-elastic behaviours are represented: hardening (*i*), perfect (*p*) and softening (*d*).

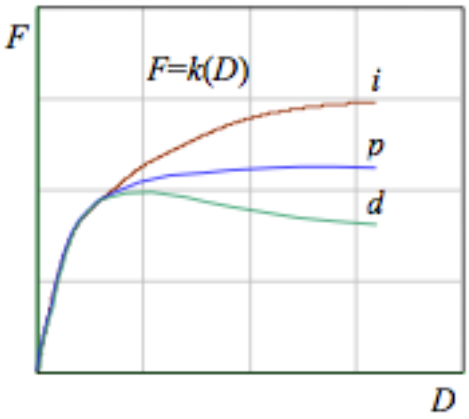

Picture 28. Capacity curves of a real system

A similar trend is gained when dealing with MDOF systems with an initial linear stroke followed by a curved non-linear one.

Finally, it is important to clarify a peculiarity of this kind of curve: it defines the structure's capacity notwithstanding any particular seismic requirement. Furthermore, once a seismic action is given, the intersection between the two would indicate the exact response of the structure to that action.

4.2.2 Linearization of the capacity curve

The previous task can be simplified by a linearization of the capacity curve by means of bilinear or trilinear approximations as shown in picture 29.

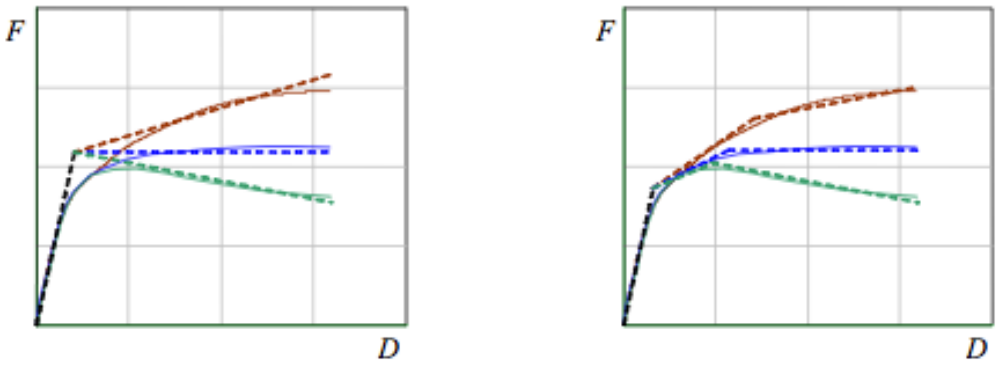

Picture 29. Bilinear (left) and trilinear (right) linearization of the capacity curve of a real system

As a general rule, we can say that the closer the linear stroke is to the real curved trend, the more accurate is the approximation.

The system behaviour can be, then, visualized as made of an initial linear elastic part until yielding and a post-elastic trend, which can be hardening, perfect or softening (picture 30). Notice that such a representation allows to immediately identify the yielding resistance F_y, the stiffness k and the post elastic stiffness $k_p = pk_e$.

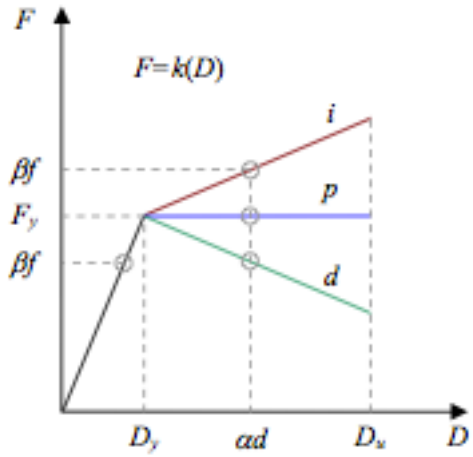

Picture 30. Schematization of hardening (i), perfect (p) and softening (d) trend

In *CSM* (ATC-40) the bilinear representation is linked to a presumed functioning point PP and it is based on a energy equivalence criterion: the first part of the bilinear curve is a line passing trough the origin and with a slope defined by the initial stiffness, while the second part is a line passing trough PP and having a slope such that the area under the bilinear curve is equal to the one under the capacity curve (see A_1 and A_2 in picture 31).

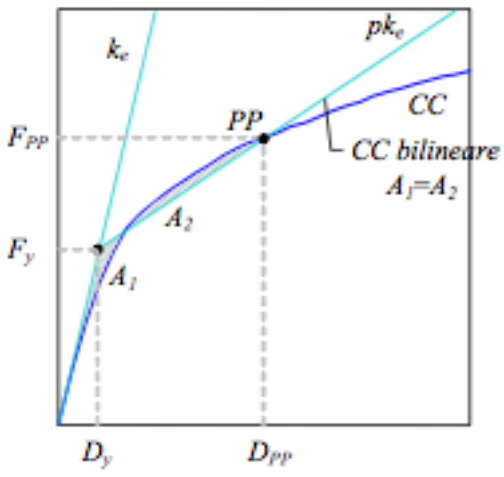

Picture 31. Representation of a bilinear capacity curve

Chapter 5

Capacity Spectrum Method (C.S.M.)

5.1 C.S.M. description

The Capacity Spectrum Method is now used in order to assess the seismic vulnerability of the analysed structure, whose performance is described by the capacity curve (see chapter 4 and 6).

In particular, this method provides general rules to get the so-called *demand spectra*, which are nothing but the curves representing possible seismic events according to the location and type of soil; once these graphs are defined, the superposition between seismic demand and structure's capacity allows to assess whether the building is safe or not.

The generic structure of such method has been reformulated by Fajfar (2000) after being introduced by Freeman: the latter is used in American regulations (ATC 40), while Italian's refer to the first one as well as Eurocode 8.

Basically, the described procedure aims at developing a unique diagram representing the earthquake demand starting from acceleration (or displacement) spectrum; actually, we deal with *pseudo-acceleration*, which is more or less equivalent to acceleration within civil engineering, especially when dealing with masonry. The result is given in terms of *Demand Spectrum*: the x axis stands for displacement, while the y axis we find the acceleration spectrum (picture 32).

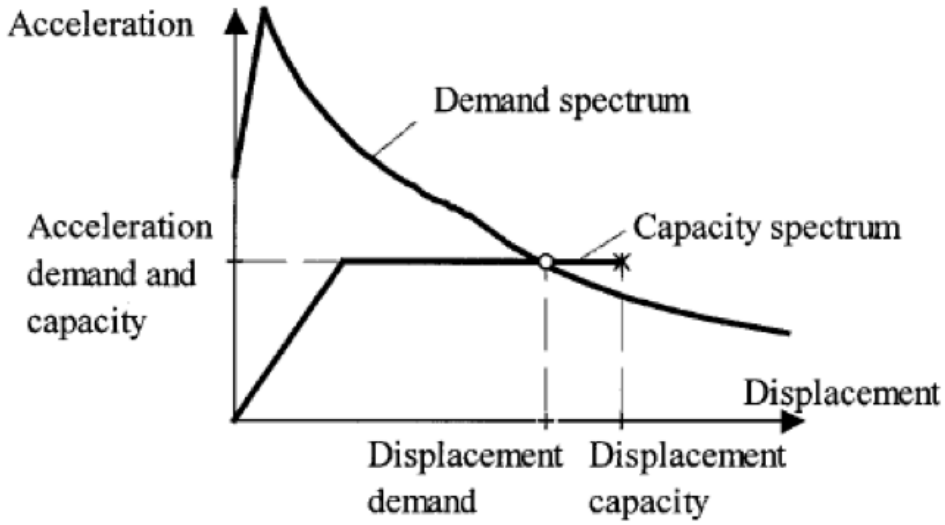

Picture 32. Capacity Spectrum Method

We notice that the period is not explicitly displayed, even if it is one of the first parameter to be set. In fact, spectra are generally defined, according to the soil type, by means of values of periods defining their shapes.

In particular, the Italian norm dictates the formulas describing the accelerograms (really close to Eurocode 8's):

$$
\begin{aligned}
&0 \le T \le T_B && S_e(T) = a_g S\left(1 + \frac{T}{T_B}(2{,}5\eta - 1)\right) \\
&T_B \le T \le T_C && S_e(T) = a_g S \cdot 2{,}5 \cdot \eta \\
&T_C \le T \le T_D && S_e(T) = a_g S \cdot 2{,}5 \cdot \eta \cdot \left(\frac{T_C}{T}\right) \\
&T_D \le T && S_e(T) = a_g S \cdot 2{,}5 \cdot \eta \cdot \left(\frac{T_C T_D}{T}\right)
\end{aligned}
\qquad (5.1)
$$

where S takes into account the stratigraphic profile of the foundation's soil, η depends on the damping (η=1 for 5% viscous damping) and a_g on the seismic category.

Moreover, there is a straight relationship between the spectral acceleration S_A and the spectral displacement S_D:

$$S_A = \left(\frac{2\pi}{T}\right)^2 S_D \quad (5.2)$$

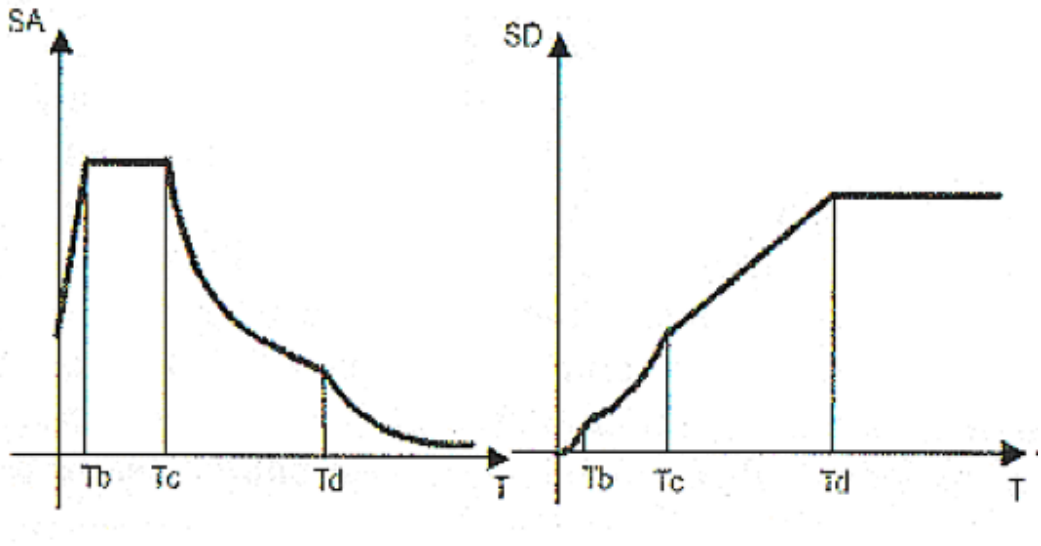

Picture 33. Relationship between spectral acceleration and spectral displacement

Furthermore, it is possible to display the capacity spectrum of the structure within a (S_A - S_D) plane by converting the forces (sum of reactions in the chosen direction) and displacements (horizontal displacement of a control point in the chosen direction). The capacity curve is nothing but the result of the non-linear static analysis; in this case, we deal with a particular kind of static analysis, which is the *pushover analysis* (Chapter 4): we are, then, able to follow the trend of the capacity of the structure even after its maximum

resistance has been reached. A further simplification can be eventually done in order to obtain a bilinear representation of the capacity curve so that only the two main behaviours are visualized: the elastic and the plastic ones.
Finally, it is necessary to reduce the demand when the structure gains a higher dissipative feature since the non-linear field is entered; in this case, the reduction can be made in two different ways: by means of an increased equivalent viscous damping coefficient (elastic over damped response spectrum) or by using reduction factors depending on the global ductility (inelastic response spectrum). Generally the Italian regulations suggest the second approach, while the first is allowed only for masonry structures.

5.2 Demand Spectra: elastic and inelastic

As previously said, the reduction of the seismic demand is due to the fact that, once a structure enters the non-linear field, it is capable of absorbing part of the energy transmitted by the earthquake: this kind of behaviour, which is cyclic, is directly linked to the concept of ductility. The latter is crucial when, due to the crossing of the elastic limit, structures get damaged and, in order to bear the seismic excitation, they rely on their own capacity of non-linear deformation instead of their strength.
This effect is taken into account by reducing the ordinates of the response spectra for acceleration and displacement; there can be different ways to do that, but all of them are based on the post-elastic features of the building (pushover analysis).

As far as this matter is concerned, we know that the elastic response spectra for acceleration and displacement for a given earthquake represent the maximum demand of absolute acceleration and relative displacement for SDOF systems characterised by indefinitely linear elastic constitutive law,

same viscous damping and variable vibration period: such curves represent the starting point for all the next steps. Besides, if the ductility is known from the beginning, we can decide to use it in order to get the spectra reduced according to the following relations:

$$R(\mu,T) = 1 + (\mu - 1)\frac{T}{T_c}, \quad T<T_C \quad (5.3)$$

$$R(\mu,T) = \mu, \quad T>T_C \quad (5.4)$$

Given the previous, the inelastic spectra with constant ductility are evaluated from the elastic ones by means of:

$$S_{Aa}(T,\mu) = \frac{S_{Ae}(T)}{R(\mu,T)} \quad (5.5)$$

$$S_{Da}(T,\mu) = \frac{\mu}{R_\mu} S_{De}(T) = \frac{\mu T^2}{4\pi^2} S_{Aa}(T,\mu) \quad (5.6)$$

where $S_{Aa}(T,\mu)$ and $S_{Da}(T,\mu)$ are, in order, the inelastic responses for acceleration and displacement.

Alternatively, we can define an equivalent viscous damping coefficient which simulate the energy dissipation of the structure; in this case, according to the Italian regulations, the elastic spectrum is modified by means of the following coefficient:

$$\eta = \sqrt{\frac{10}{5+\xi}} \quad (5.7)$$

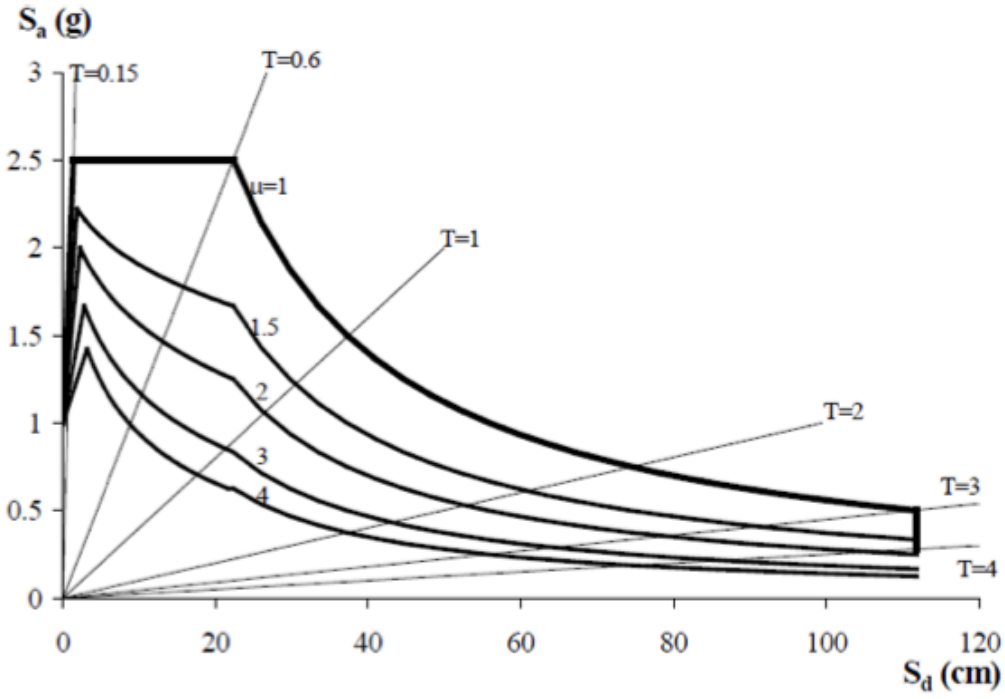

Picture 34. Inelastic response spectra for constant ductility in S_D-S_A plane

where ξ stands for the percentage of the visco-elastic damping with respect to the critical value: generally, the 5% is assumed for RC and masonry structures so that η=1.

As we will see in next paragraphs, the method implied for the current case study is the second one.

5.3 Fajfar's method according to the new seismic regulation

The main goal of the method is the determination of the maximum displacement of the structure after a specific seismic event has occurred by means of the superposition of the capacity curve and the reduced spectrum.

A brief explanation of the procedure is now provided in order to better understand which are its key steps:

1. *Evaluation of Γ and m*:* they are called participation coefficient and participation mass and both are referred to the control node, which is generally taken as the centre of mass of the highest floor; from a numerical point of view, we need to perform an elastic analysis by setting a modal forces field (or, more often, forces proportional to masses times heights) and to evaluate the displacement vector Φ so that:

$$\Gamma = \frac{\sum m_i \Phi_i}{\sum m_i \Phi_i^2} \quad (5.8)$$

$$m^* = \sum m_i \Phi_i \quad (5.9)$$

2. *Pushover analysis:* once the force distribution is assigned, a pushover analysis is performed obtaining a base shear-control node's displacement curve. Such curve would be stopped once the strength is decreased by 20%.
3. *Bilinear simplification 1:* assuming that the elastic part of the bilinear curve crosses the capacity curve when 70% of strength is reached, we can even define the equivalent stiffness as:

$$k^* = \frac{F_{70\%}}{d_{70\%}} \quad (5.10)$$

4. *Bilinear simplification 2:* the flat part of the bilinear is given by the value of F_y, which is computed by setting the equality between the area under the bilinear and the area under the pushover curve:

$$F_y = \left(d_u - \sqrt{d_u^2 - 2\frac{Area}{k^*}} \right) k^* \quad (5.11)$$

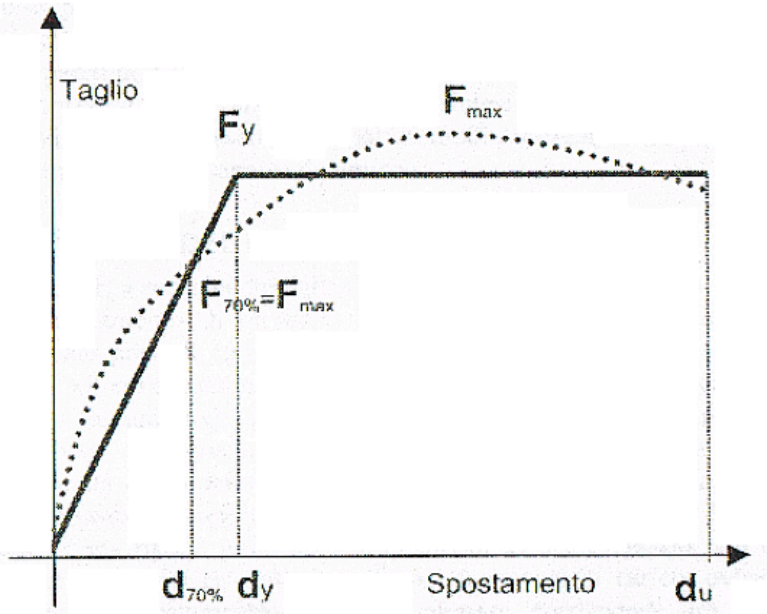

Picture 35. General scheme for the evaluation of the equivalent bilinear curve

5. *Normalization of the bilinear curve:* the bilinear curve is normalized by dividing both force and displacement by Γ and getting the values F^*_y and d^*_u.

6. *Seismic demand in AD format:* starting from the usual acceleration spectrum (obtained once soil and location parameter has been set) in acceleration versus period format, inelastic spectrum is determined in acceleration-displacement (AD) format. Moreover, for an elastic SDOF system we can evaluate the elastic displacement S_{De} correspondent to the elastic acceleration S_{Ae} by means of the 5.2, while for an inelastic SDOF system the acceleration spectrum S_{Aa} and the displacement spectrum S_{Da} are evaluated in the 5.5 and 5.6. Starting from the elastic design spectrum and using the previous equations, we get the elastic design spectrum in the AD format; eventually, its reduction is performed by means of $R(\mu,T)$ (see 5.3 and 5.4) coefficients.

7. *Performance evaluation:* expected performance is assessed by superposition of seismic demand and capacity curve so that a comparison between their displacement values is possible.

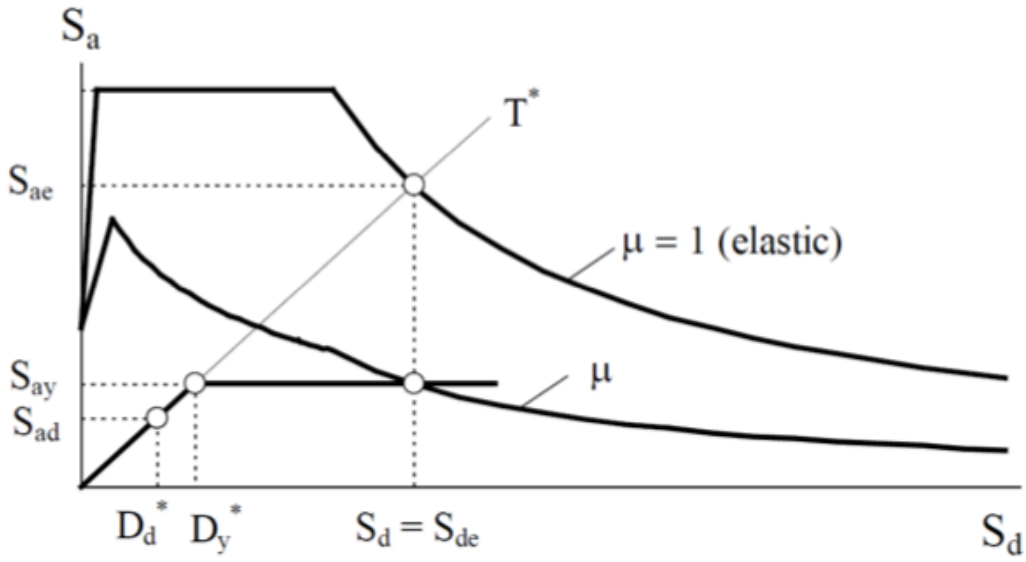

Picture 36. Elastic and inelastic spectra and bilinear capacity curve

Looking at picture 36, we see that T^* represents the period associated with the bilinear capacity curve:

$$T^* = 2\pi\sqrt{\frac{m^*}{k^*}} \quad (5.12)$$

The displacement demand for the inelastic spectrum can be evaluated according to T^* eventually getting d^*_{max} so that the maximum displacement required for the real system is:

$$d_{\max} = \Gamma d^*_{\max} \quad (5.13)$$

Chapter 6

Structural modelling and analysis

6.1 Software and main assumptions

The analysis of the structure is performed by means of a mathematical model the finite element theory; for this purpose software Straus7 is used, which is the European equivalent of the American Strand7, developed by Strand7 Pty Ltd. The peculiarity of such software is being able to perform different kind of analysis suitable for almost any engineering field.
In this particular case some assumptions have been initially set:

- non-structural masses are neglected
- foundations are simulated as non linear spring that do not resist traction in order to better describe the real behaviour of the walls under horizontal loads
- masonry has been defined as a homogeneous material whose characteristics depend on those of mortar and stone
- Mohr-Coulomb collapse criterion has been selected to represent masonry.

The latter will be better clarified in the next paragraph.

6.1.1 Mohr-Coulomb collapse criterion

In order to avoid some issues related to the representation of materials by means of certain collapse criteria such as Turnsek and Cacovic's [Turnsek and Cacovic, 1971], new formulations were provided and, in particular, Mohr-Coulomb criterion is still one of the most used.
This kind of method is really useful since it takes into account a failure due to slipping and not only to diagonal cracking: such a behaviour is, in fact, the one we should expect during experimental tests on masonry.

Mohr-Coulomb criterion evaluates masonry's shear resistance as follows:

$$|\tau| = c + \mu\sigma \quad (6.1)$$

where c and μ are cohesion and friction coefficient for masonry, while σ and τ are normal and tangential stresses. As specified in the previous relation, the criterion itself assumes that the slipping happens when, at least on one plane, the modulus of the tangential stress τ is equal to a limit value, which is linearly dependent to normal stress.
Such a criterion is strongly linked to the value of the normal stress σ and this aspect is one of the main differences from other methods.

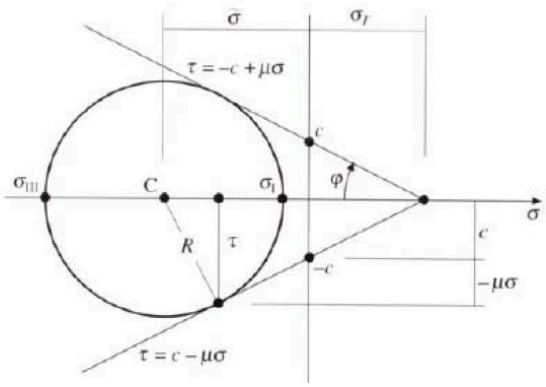

Picture 37. Limit lines and tangent circle according to Mohr-Coulomb

As shown in picture 37, the Coulomb relationship can be represented within the Mohr plane by means of three lines whose equations are:

$$\sigma_{II} - \sigma_I = \pm\sigma_s \quad \sigma_{III} - \sigma_I = \pm\sigma_s \quad \sigma_{III} - \sigma_{II} = \pm\sigma_s \quad (6.2)$$

where σ_{I} , σ_{II} and σ_{III} are principal stresses and σ_{s} is the yielding stress. The limit stress states are those referring to the maximum circles, which are tangent to the two lines in picture 37. Recalling that the maximum radius is:

$$R = \frac{(\sigma_I - \sigma_{III})}{2} \quad (6.3)$$

we can geometrically express the criterion in the form:

$$R = (\sigma_T - \tilde{\sigma})\sin\varphi \quad (6.4)$$

where:

$$\tilde{\sigma} = \frac{(\sigma_I + \sigma_{III})}{2} \quad \text{and} \quad \sigma_T = \frac{c}{\tan\varphi} \quad (6.5)$$

so that we can finally write:

$$\frac{1}{2}(\sigma_I - \sigma_{III}) = \frac{1}{2}(\sigma_I + \sigma_{III})\sin\varphi + \cos\varphi \quad (6.7)$$

Differently form Tresca criterion, Coulomb's makes the collapse depend on the hydrostatic tension throughout the term $(\sigma_I + \sigma_{II})$: the two of them are equal if and only if the angle of friction φ is null.

Furthermore, in the space of principal stresses (0, σ_I , σ_{II} , σ_{III}) the condition must be expressed by all its possible combinations:

$$\begin{aligned}
\sigma_{II} - \sigma_I &= \pm 2c\cos\varphi \mp (\sigma_I + \sigma_{II})\,sen\varphi \\
\sigma_{III} - \sigma_I &= \pm 2c\cos\varphi \mp (\sigma_I + \sigma_{III})\,sen\varphi \\
\sigma_{III} - \sigma_{II} &= \pm 2c\cos\varphi \mp (\sigma_{II} + \sigma_{III})\,sen\varphi
\end{aligned} \qquad (6.8)$$

The previous relations are the equations of six planes whose envelope is a pyramid whose vertex's coordinates are σ_I ,= σ_{II} = σ_{III} = σ_T and whose axis is the hydrostatic one.

When dealing with biaxial stress states (σ_{III} = 0), the equations become:

$$-\frac{\sigma_I}{\sigma_c} + \frac{\sigma_{II}}{\sigma_t} = 1, \quad \frac{\sigma_I}{\sigma_t} - \frac{\sigma_{II}}{\sigma_c} = 1, \quad \sigma_I = -\sigma_c = \sigma_t, \quad \sigma_{II} = -\sigma_c = \sigma_t, \qquad (6.9)$$

once we set:

$$\sigma_t = \frac{2\,c\,\cos\varphi}{1+sen\,\varphi} \quad \text{e} \quad \sigma_c = \frac{2\,c\,\cos\varphi}{1-sen\,\varphi} \qquad (6.10)$$

as traction and compression strengths.

In this case the envelope of the six lines gives an irregular hexagon, which is the intersection between the pyramid's lateral surface and the σ_{III} = 0 plane.

It is, then, useful to notice how the Coulomb slipping domain, being defined throughout two parameters (c and φ), is actually able to describe the different traction and compression resistances; besides, when φ = 0, we get σ_T = σ_C and the hexagon coincides once again with Tresca's. Finally, due to the independence from the intermediate principal tension σ_{II}, the criterion gives the same monoaxial and biaxial compressive strength.

6.2 Structural model

As far as the case study is concerned, two different kind of models have been created: a 3D scheme, useful for a clear visualization of the structure as a whole, and 2D representations of the main internal and external walls, at which the analysis is straight directed.
As previously said, the modelling for masonry structures usually refers to a homogeneous material whose elastic properties depend on those of mortar and stone.
In order to describe the global behaviour of the walls, a dense discretization is performed. To this purpose the finite elements selected to create a virtual model for masonry in Straus7 are basically bidimensional plate elements (quad elements, 4 nodes); in particular, 1800 plates on average make up each wall, thus having mean dimensions of 40 cm x 30 cm. In addiction, each plate has been given 50 cm thickness given that the primary investigation on field pointed out that the walls' thickness range was between 30 cm and 65 cm.
Moreover, beam elements (2nodes) are used to represent the curbstone and for the architraves: their cross section has been equally set to 30 cm x 40 cm according to the collected data.

6.2.1 Materials modelling

Given that Strus7 materials database does not provide a suitable option for masonry, it is necessary to set its main properties and manually insert them within the model; in particular, masonry is here modelled as a continuous and homogeneous equivalent material to which certain properties has been given according to those of mortar and stone.

Moreover, assuming a Mohr-Coulomb collapse criterion (see §§6.2), we can evaluate the angle of friction φ and cohesion c as follows:

$$\sin\varphi = \frac{f_c - f_t}{f_c + f_t} \quad \text{and} \quad c = \frac{f_c f_t}{f_c - f_t}\tan\varphi \qquad (6.11)$$

where both of them are expressed in terms of monoaxial compressive and tensile strength.
According to data collected from literature (see §§3.2), we assume:

- f_{mc} = 5,5 MPa
- f_{mt} = 0,55 MPa
- ν = 0,2
- γ =1800 kg/m^3
- E = 2000 MPa

leading to:

$$\varphi = 55° \quad \text{and} \quad c = 0{,}5 \text{ MPa}$$

As far as the beam elements are concerned, since it was not possible to check the real presence of curbstones, Concrete C20/25 (according to NTC 2008) has been selected in order to idealize a sort of stiffening at slab's level. For further details see table 1.

The reason why concrete has been used is basically due to the evidences reported after an initial overlook of the structure.

classe	C20/25
f_{ck}	20 MPa
E_{cm}	30000 MPa
f_{ctm}	2.21 MPa
f_{ctk}	1.55 MPa
f_{cfk}	1.86 MPa

Table 1. Concrete properties

6.2.2 2D Model

In this case the kind of bidimensional element used for modelling is a Plate/Shell element; in order to perform a 2D pushover analysis, certain constraints have to be set: in particular, for each wall, rotations in the three directions as well as translation in the plane orthogonal to the wall's one are fixed.
Besides, all of the 2D walls have been defined with a number of lateral nodes that are supposed to be matched when dealing with the 3D scheme.

The following paragraphs describe the main steps that lead to the final analysis.

6.2.3 Load analysis and model of the actions

The first step towards a global analysis is the evaluation of loads acting on the structure; they can be divided into:

- Gravity (vertical) actions: permanent and variable
- Seismic (horizontal) forces

Thus, for each wall two different load layers are created in Strus7 so that, during the real analysis, it is possible to apply different load increment to different kind of loads.

6.2.3.1 Gravity actions

First of all, the self-weights of masonry plates and concrete beams are automatically considered by setting the option *Gravity* (see picture 38) on Straus7 and indicate the value of 9,81 m/s^2 along the vertical axis (y axis in this case).

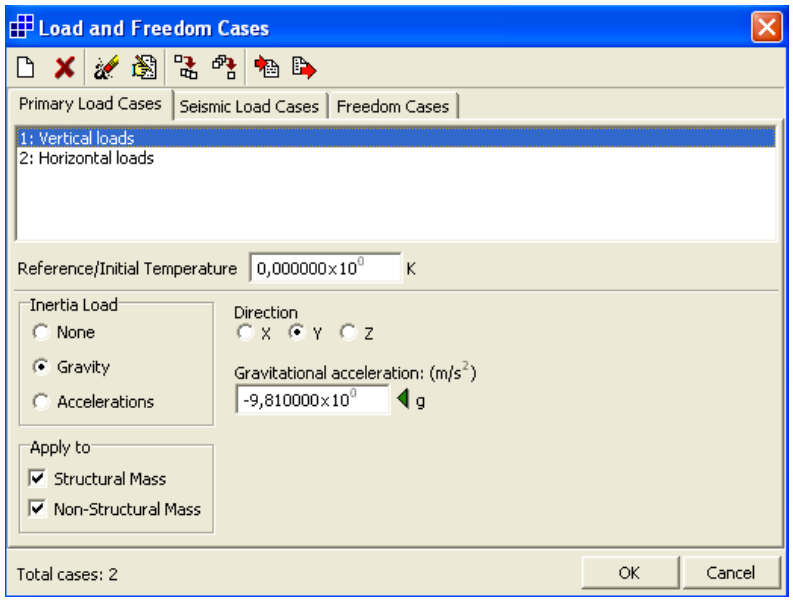

Picture 38. Gravity option window

Notwithstanding the reliability of the software, some handmade verification are done in order to get a reasonable comparison of the masses; the results, which are highly close to Straus' are collected in table 2.

	Total self weight [kg]
Front Wall	204091
Right Handside Wall	444716
Left Handside Wall	518352
Back Wall	234486

Table 2. Self weight for each wall

Then slab's weights have to be defined and to do so, we choose:

- 450 kg/ m^2 as dead load
- 200 kg/ m^2 as variable load

These values have been selected according to the most likely kind of slab we found during the primary investigation on field; a literature's in-depth analysis has eventually given such results.

Moreover the initial examination of the site was aimed at taking note of the disposition of the timber beams for each slab in order to perform a detailed load computation. In fact, given the orientation of the slabs, we are able to understand which wall would bear which load. Pictures 39,40 and 41 display the results of the preliminary study.

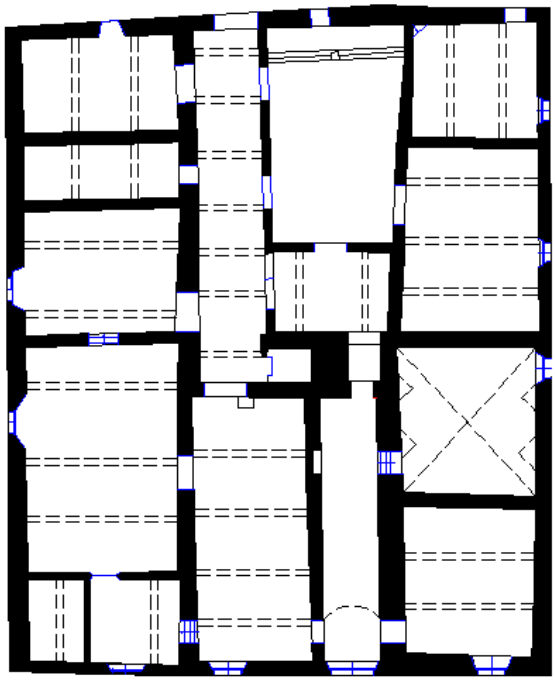

Picture 39. Ground floor slab disposition

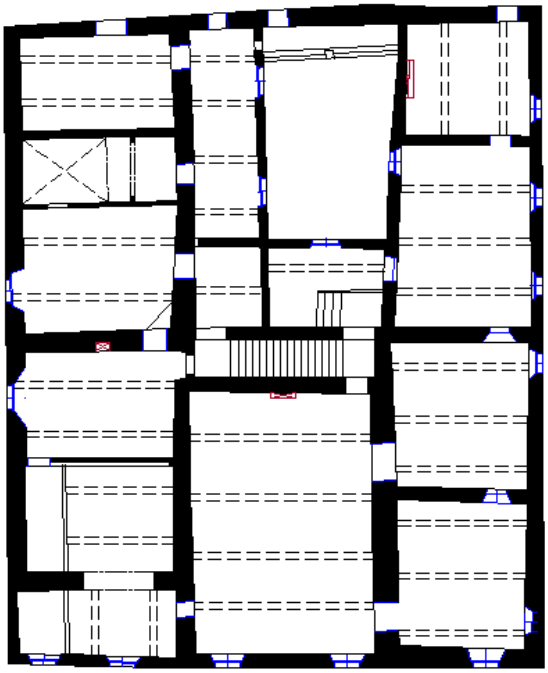

Picture 40. Raised ground floor slab disposition

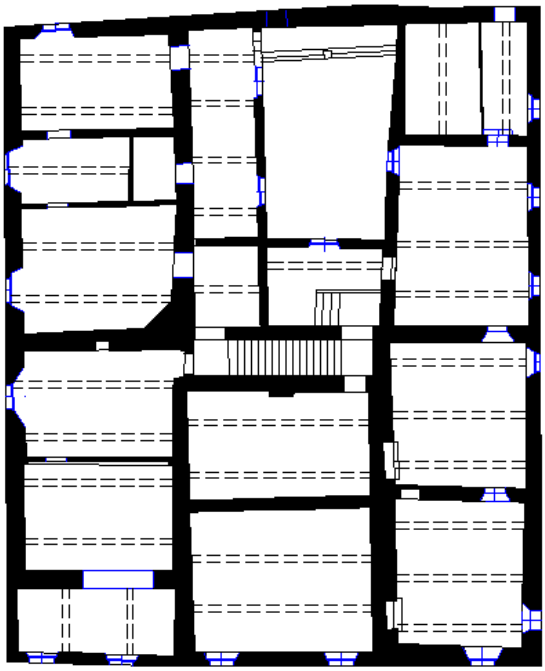

Picture 41. First floor slab disposition

Once we know how to distribute loads, getting through a bit of hand calculation, we get:

	Front Wall	Right Handside Wall	Left Handside Wall	Back Wall	
Ground Floor	0,11	0,38	0,63	0,14	**SLAB LOAD [kN/m]**
Raised Ground Floor	0,08	0,5	0,75	0,14	
First Floor	0,08	0,5	0,8	0,14	

Table 3. Slab Load result

Notice that top load has been neglected since roof is always made by wood trusses, which discharge their load on trasversal walls.

According to NTC08 par. 2.5.3., the seismic combination to be used is:

$$E + G_1 + G_2 + \psi_{21} Q_{k1} \quad (6.12)$$

Given that E is null in the vertical direction and being ψ_{21} = 0,3 for residential use, we are able to evaluate the total gravity load for each slab:

	Distributed seismic weight along the slab [kN/m]	
Front Wall	Raised Ground Floor	6,17
	First Floor	6,17
	Roof	0,00
Right Handside Wall	Raised Ground Floor	38,56
	First Floor	38,56
	Roof	0,00
Left Handiside Wall	Raised Ground Floor	58,78
	First Floor	65,18
	Roof	0,00
Back Wall	Raised Ground Floor	11,35
	First Floor	11,35
	Roof	0,00

Table 4. Vertical load over the slabs

6.2.3.2 Seismic forces

In order to perform a pushover analysis, horizontal forces have to be applied to each slab level; in particular, these values have to be calibrated according to certain selected distributions. As far as this particular case is concerned, forces proportional to product between mass and height are applied.

The first step towards such result is a *natural frequency analysis*, which is needed in order to define the displacement vector Φ (see §§5.3): the latter is used to compute the *participation mass* m^* and the *participation coefficient* Γ. In particular, three nodes (generally the centre of mass for each slab) are selected for each wall and relative displacements are taken for the first vibration mode; then, they are all normalized with respect to the upper floor's. Recalling the m^* and Γ formulas (see5.8 and 5.9), the results are summarized in table 5.

		Φi [m]	Φi normalized[m]	m* [kg]	Γ
Front Wall	Raised Ground Floor (Node 2029)	0,0018	0,6	166173,47	1,18
	First Floor (Node 3528)	0,0028	0,93		
	Roof (Node 389)	0,003	1		
Right Handside Wall	Raised Ground Floor (Node 1677)	0,0011	0,39	311142,03	1,25
	First Floor (Node 561)	0,0025	0,89		
	Roof (Node 144)	0,0028	1		
Left Handiside Wall	Raised Ground Floor (Node 1736)	0,0019	0,79	400734,52	1,28
	First Floor (Node 962)	0,0017	0,71		
	Roof (Node 258)	0,0024	1		
Back Wall	Raised Ground Floor (Node 1912)	0,0015	0,48	172936,21	1,25
	First Floor (Node 1924)	0,0026	0,84		
	Roof (Node 1936)	0,0031	1		

Table 5. Main results of the modal analysis

Besides, modal analysis allows determining even the frequency of the first vibration mode in the chosen direction so that the correspondent period T_1 can be evaluated recalling that:

$$T = \frac{1}{f} \quad (6.13)$$

Once the period is known, we look $S_D(T_1)$ up in the elastic spectrum for displacement; finally, according to the §§7.3.3.2 of the NTC08, we can compute:

$$F_h = S_D(T_1) W \frac{\lambda}{g} \quad (6.14)$$

where F_h is the overall horizontal force which has to be distributed along the building's height, W is the total weight of the structure, λ is a coefficient depending on the number of floors and set to 0,85 (if $T_1 < 2T_C$) and g is nothing but the gravity acceleration (9,81 m/s^2).

Given F_h, eventually we get:

$$F_i = F_h \frac{z_i W_i}{\sum_j z_j W_j} = F_h \alpha \quad (6.15)$$

where z_i and W_i are the heights and weights of each floor. In particular, the previous relation is the one describing the application of horizontal forces that are proportional to the product between mass and height; moreover, this approach (named *Gruppo 1* within the Italian regulations) is to be used only if the percentage of participant mass is higher than 75%: according to the results shown in tables 2 and 5, such condition is always verified.
Given all the previous, we get F_i values for the 4 walls (table 6).

	Distributed horizontal load along the slab [kN/m]	
Front Wall	Raised Ground Floor	0,0030
	First Floor	0,0074
	Roof	0,0036
Right Handside Wall	Raised Ground Floor	0,0059
	First Floor	0,0136
	Roof	0,0056
Left Handiside Wall	Raised Ground Floor	0,0063
	First Floor	0,0178
	Roof	0,0052
Back Wall	Raised Ground Floor	0,0036
	First Floor	0,0069
	Roof	0,0057

Table 6. Design horizontal forces

Once we apply all the above loads, the non-linear static analysis can be performed by setting a series of load increments, which are basically multipliers to be used for horizontal forces: in this way the structure is gradually pushed to collapse and the capacity curve is obtained (Pictures 42, 43, 44 and 45).

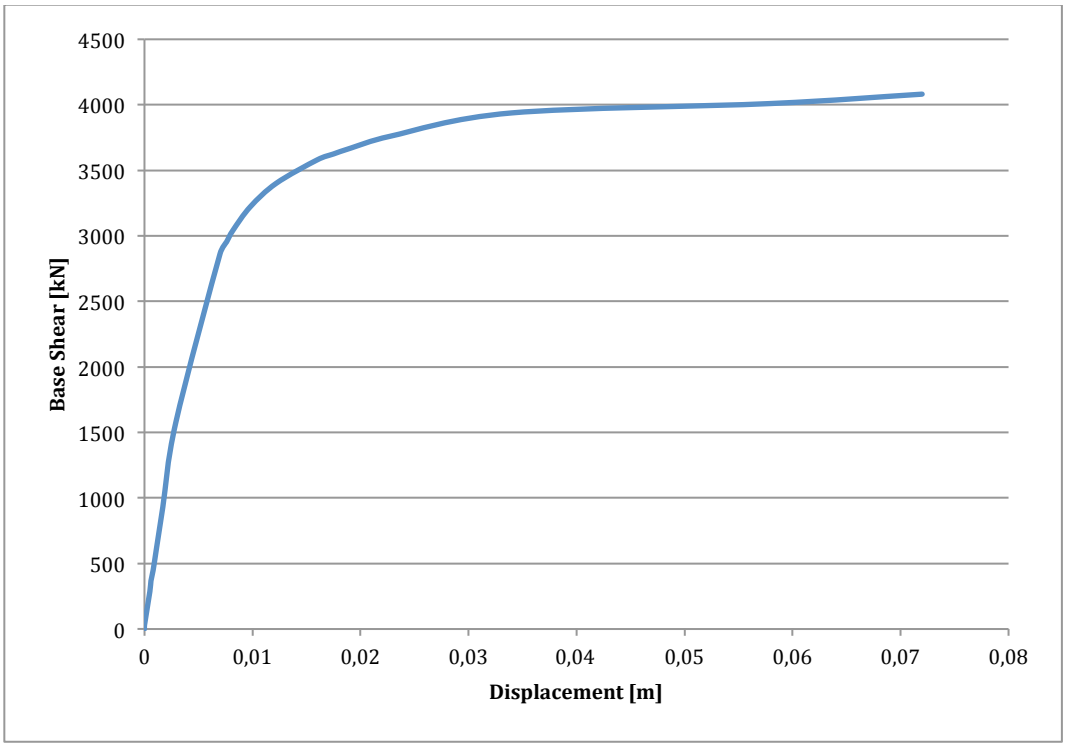

Picture 42. Front wall capacity curve

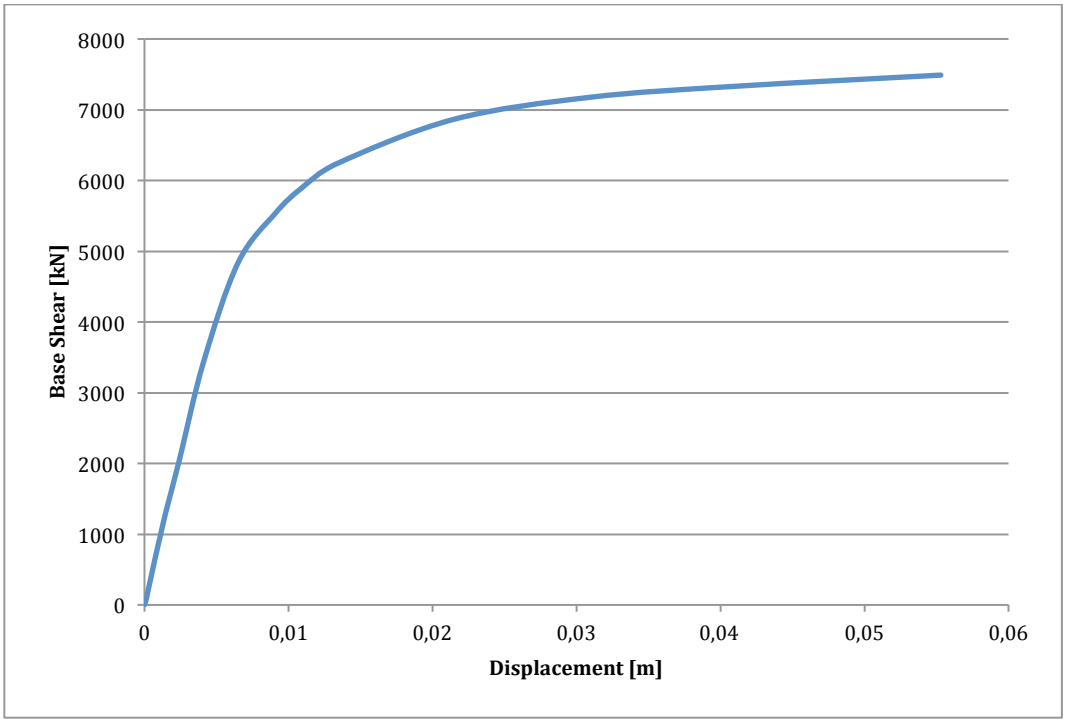

Picture 43. Right handside wall capacity curve

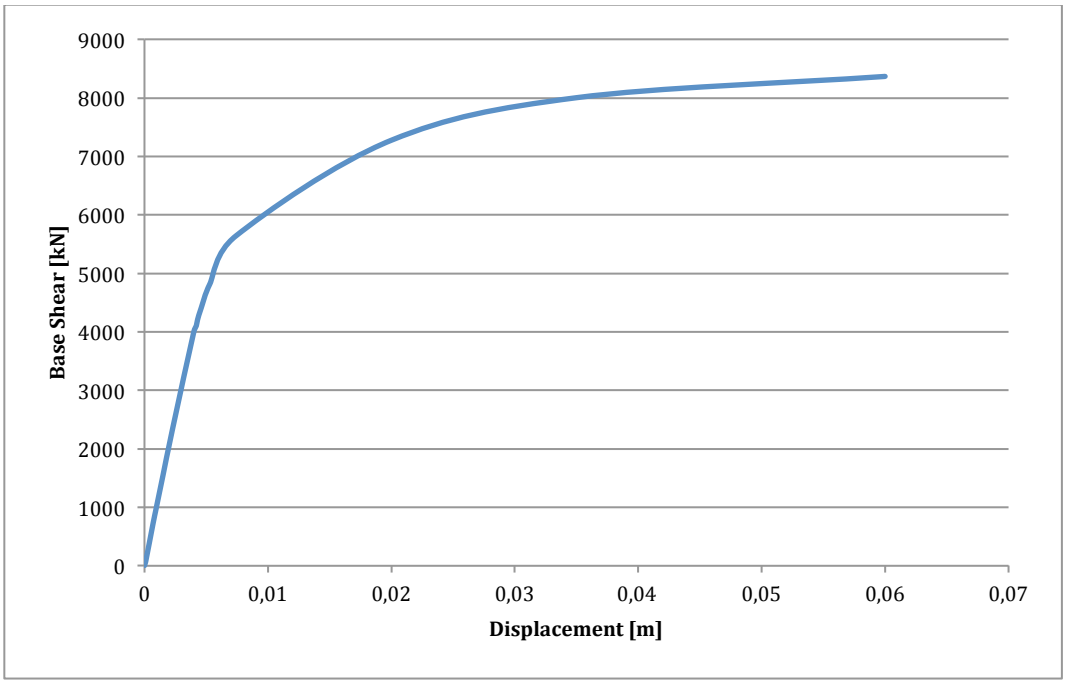

Picture 44. Left handside wall capacity curve

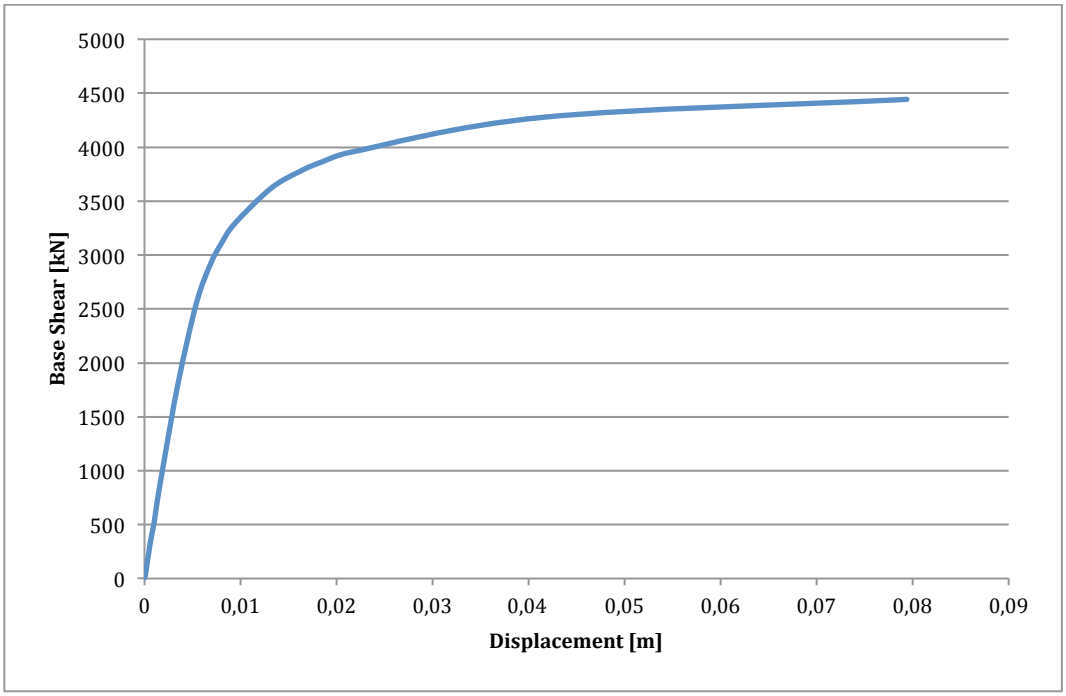

Picture 45. Back wall capacity curve

All the shown capacity curves represent the real MDOF system so that, in order to be compared to the design spectra, they need to be changed into a SDOF representation: this goal is achieved by means of the participation coefficient *Γ*, as explained in §§5.3, which is going to physically reduce the original curves. Moreover, a further simplification can be done redefining the curve as a *bilinear* curve: the procedure, which has been described in §§4.2.2, is based on areal equality and its results are provided in pictures 46, 47, 48 and 49. Notice that all these pictures straight represent the SDOF bilinear graphs.

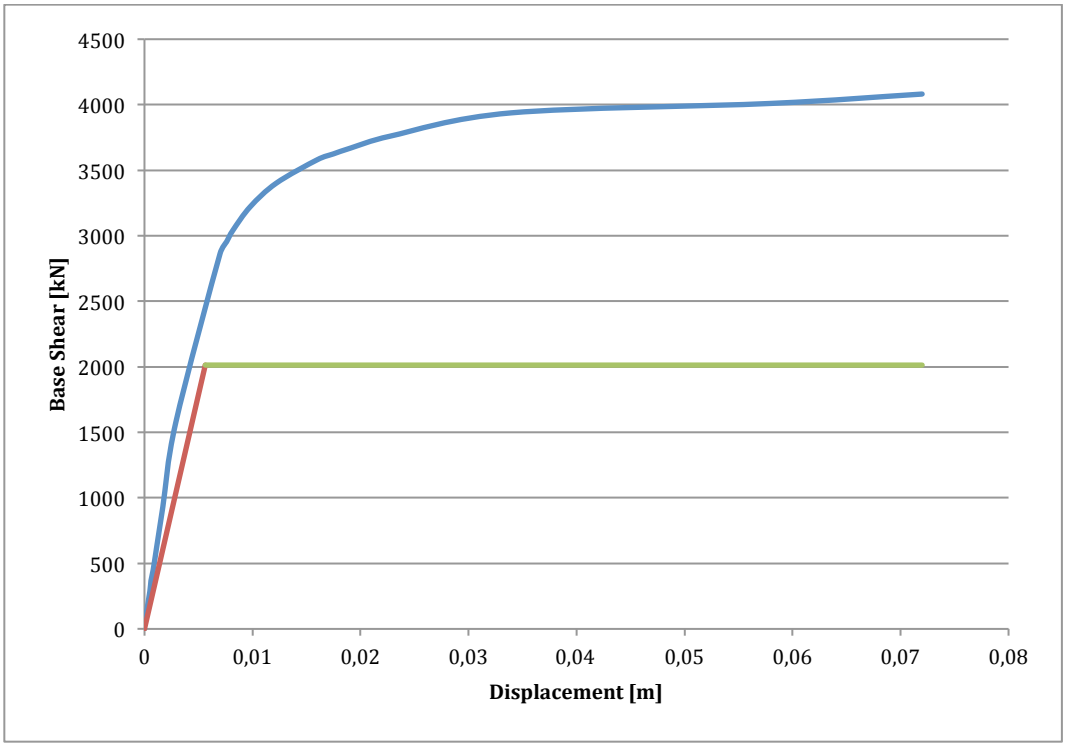

Picture 46. Front wall: MDOF and SDOF bilinear capacity curves

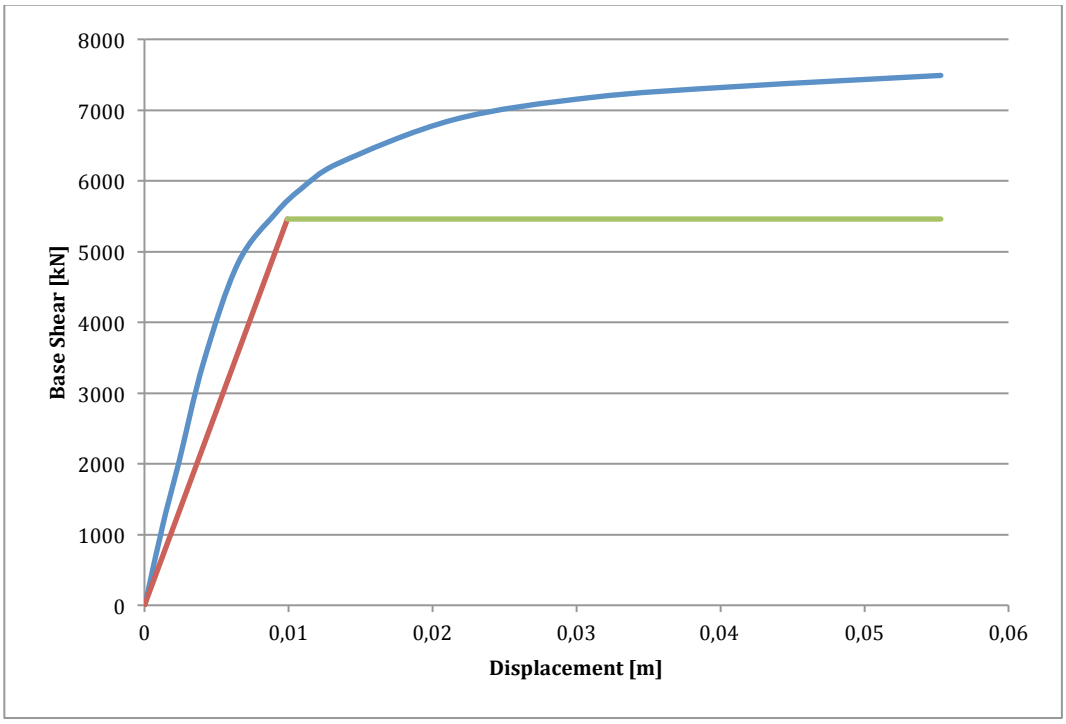

Picture 47. Right handside wall: MDOF and SDOF bilinear capacity curves

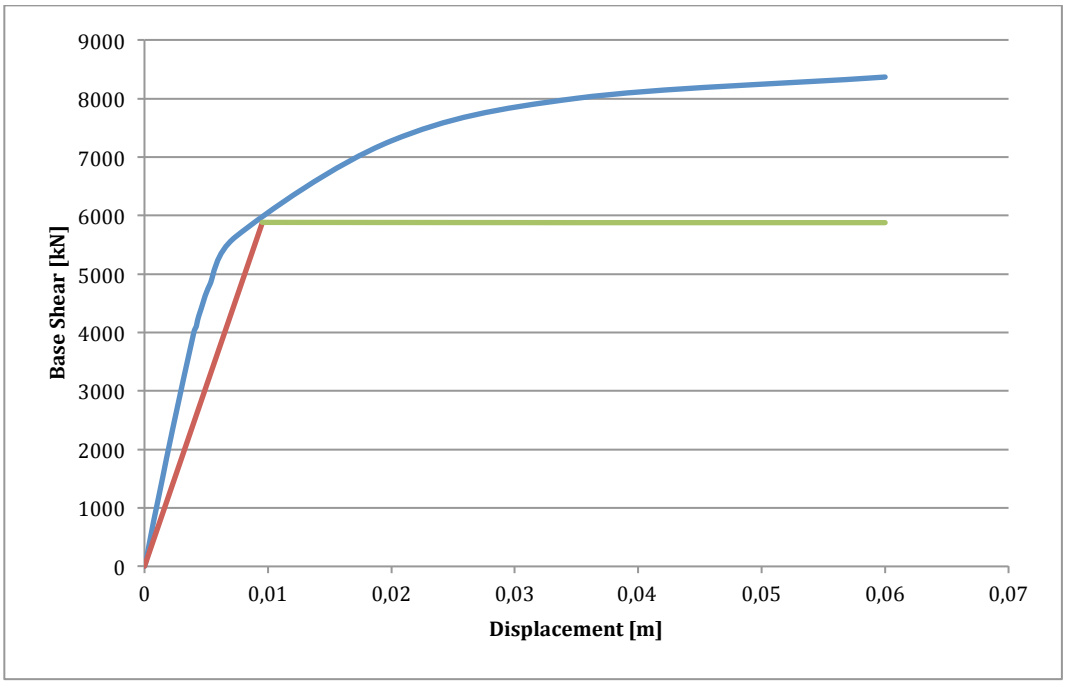

Picture 48. Left handside wall: MDOF and SDOF bilinear capacity curves

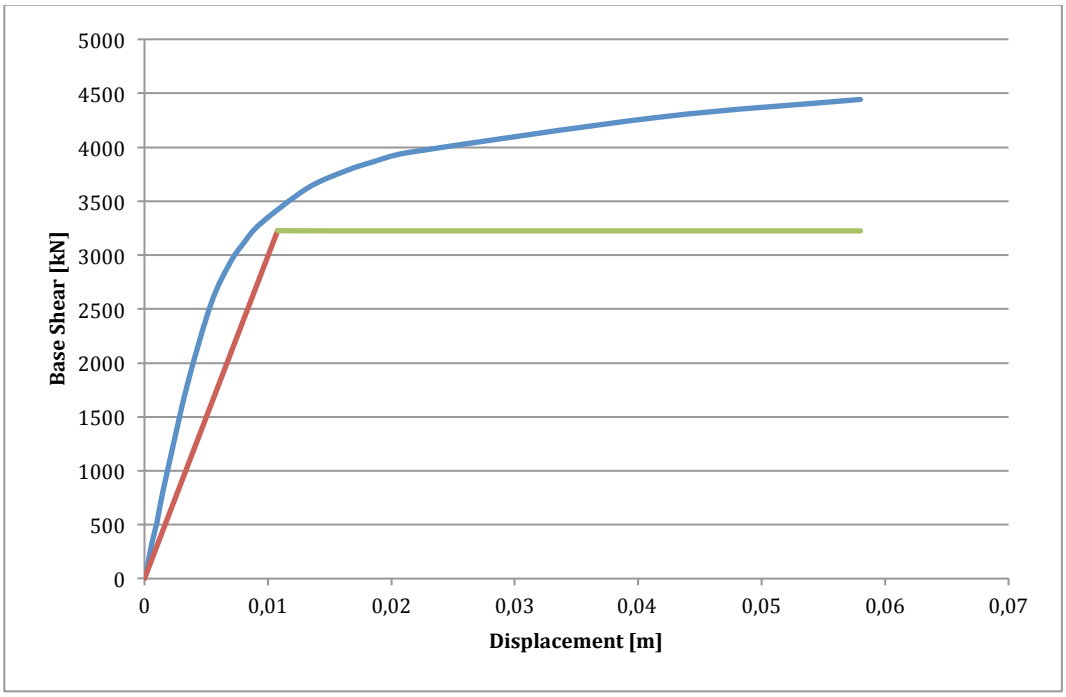

Picture 49. Back wall: MDOF and SDOF bilinear capacity curves

Finally, we can display the results of the non-linear static analysis even in terms of vertical stresses and deformed shape, as shown in pictures 50, 51, 52 and 53.

6.3 Design spectra

In order to assess the seismic vulnerability of the structure, seismic spectra have to be defined, but, firstly, we should decide which kind of verification to be done so that needed parameters are set. In this case, according to Italian NTC08, two different circumstances are analysed: one for the ultimate limit state, which is the *life protection limit state* (SLV) and one for the service limit state, which is the *damage* (*loss*) *limit state* (SLD).

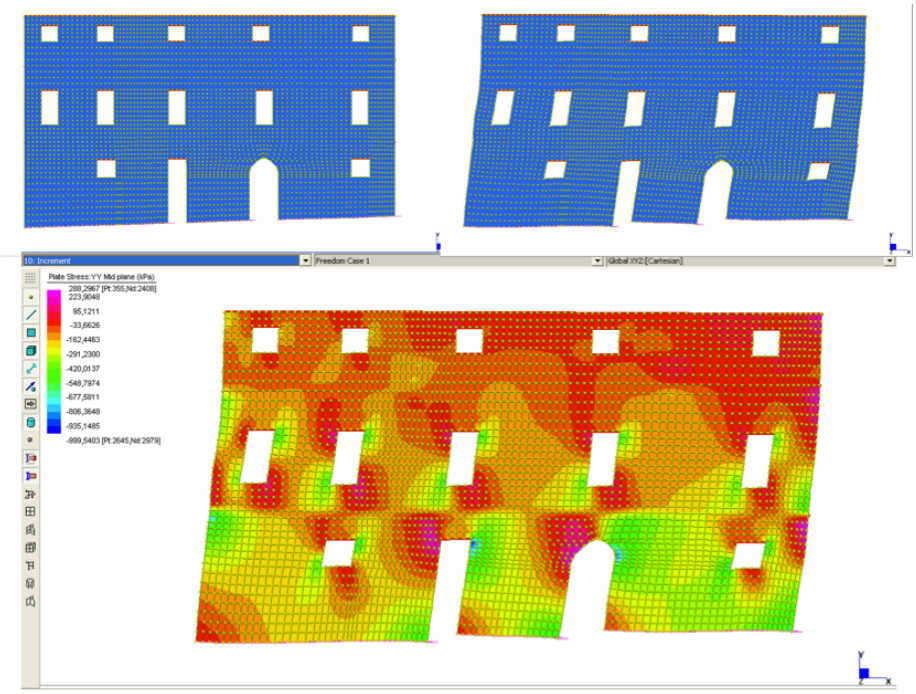

Picture 50. Front wall YY stress and deformed shape

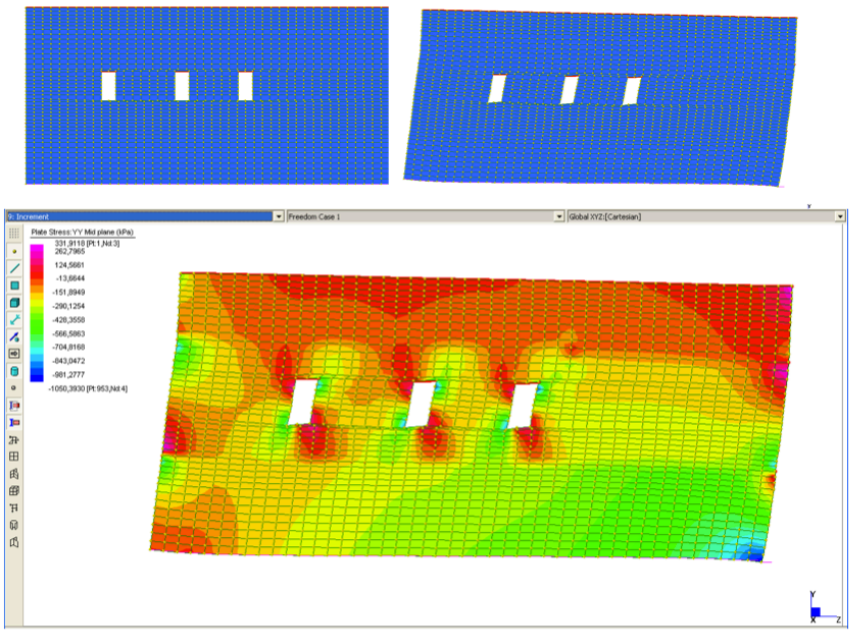

Picture 51. Right handside wall YY stress and deformed shape

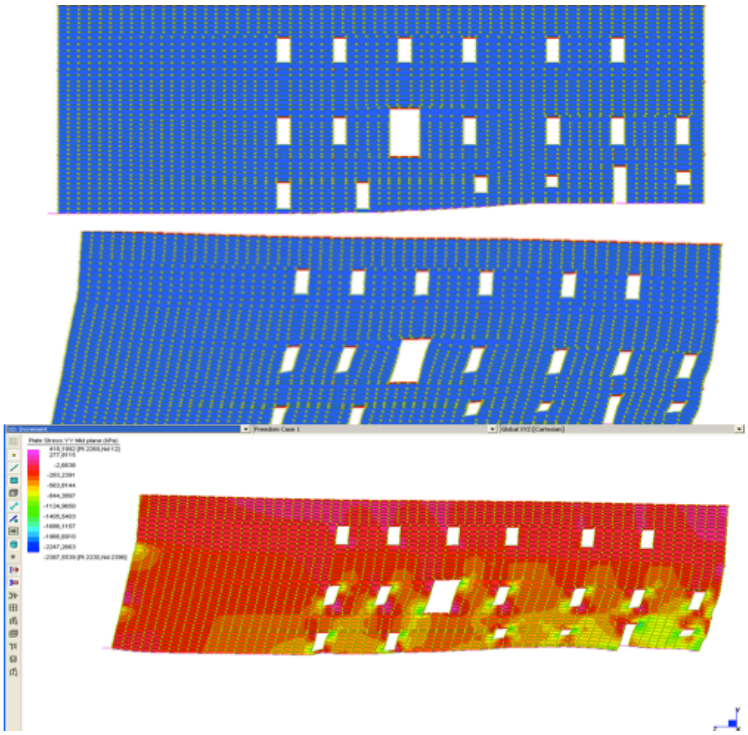

Picture 52. Left handside wall YY stress and deformed shape

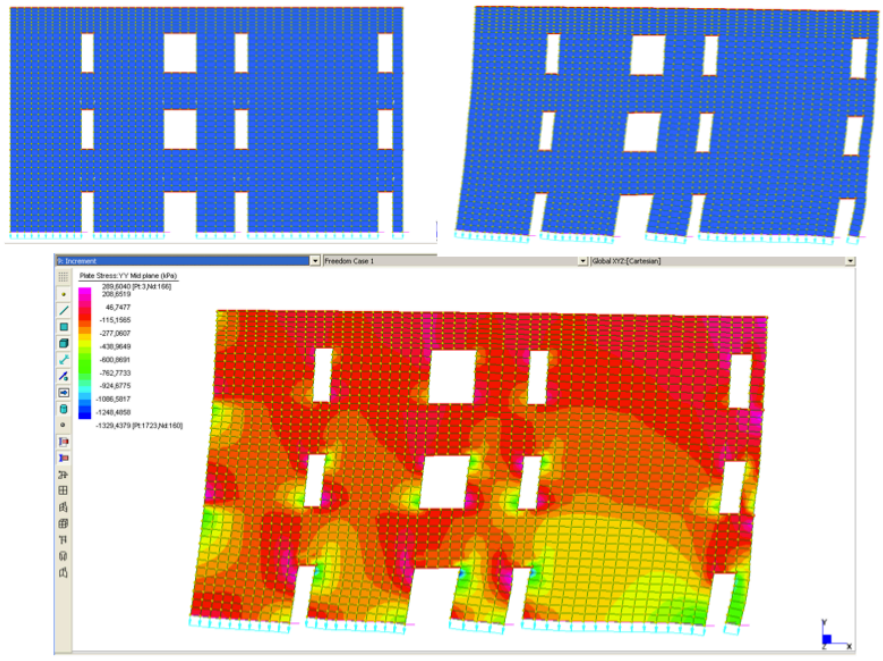

Picture 53. Back wall YY stress and deformed shape

Both of them are associated to a certain probability of being exceeded (P_{VR}) within the reference period:

$$V_R = V_N C_U \quad (6.16)$$

where V_N is the nominal life of the construction (number of years during which the structure, if subjected to ordinary maintenance, should be used for its initial purpose) and C_U is the usage coefficient depending on the class of use (normal presence of people).
Moreover, according to the site location and to the soil main characteristics, some factors are defined (Table 7).

Latitude [°]	Longitude [°]	Class of use	Vn [years]	Cu	Vr [years]	Soil category	Topographic category
43,420238	11,905635	II	50	1	50	A	T1

Table 7. Initial parameters setting

Table 7 shows that the building is located on a A category soil, which is a very rigid soil or characterised by emerging rocky terrains; besides, the T_1 topographic category means a level land or hill sides and reliefs with average slope $i \leq 15°$.
Finally, the last parameter we need before developing the elastic spectrum, is the behaviour factor q; according to NTC08 7.8.1.3, for existing masonry structures we should evaluate:

$$q_0 = 2{,}0 \frac{\alpha_u}{\alpha_1} \quad (6.17)$$

where q_0 is the maximum value for the structure's factor depending on the expected ductility and on the type of construction, while α_u/α_1 is a coefficient based on the horizontal seismic force multipliers and, in this case, set to 1,5.
The behaviour factor will be then:

$$q = q_0 K_R \quad (6.18)$$

and K_R set to 0,8 for building with irregular height distribution; the overall q is then 2,4, which is a quite common value for existing structures.
Now we have all the parameters we need in order to use the Excel spread sheet *Spettri – NTC ver.1.0.3.* released by the Italian *Consiglio Superiore dei Lavori Pubblici*: such tool allow to immediately display the elastic spectra for SLD and SLV as shown in pictures 54. Anyway, for a more precise analysis, same curves have been manually obtained by means of relationship 5.1. Notice, that, as regulations clearly say (§§3.2.3.4 and 7.3.7.1; §§3.2.3.5), the elastic spectrum is to be used for SLD, while for ultimate limit state (SLV) a reduction needs to be applied and the relative inelastic spectrum (picture 55) is defined in order to take into account the dissipative capacity of the structure: such reduction can be obtained by substituting η with $1/q$ in formulas 5.1.
Before making a comparison between demand and capacity, we need to represent both graphs in the same plane, namely acceleration-displacement; following the relationships 5.2 and 5.8, the capacity curve and the design spectra are modified in order to be represented in the same way. The results of this are shown in pictures 56, 57, 58 and 59.

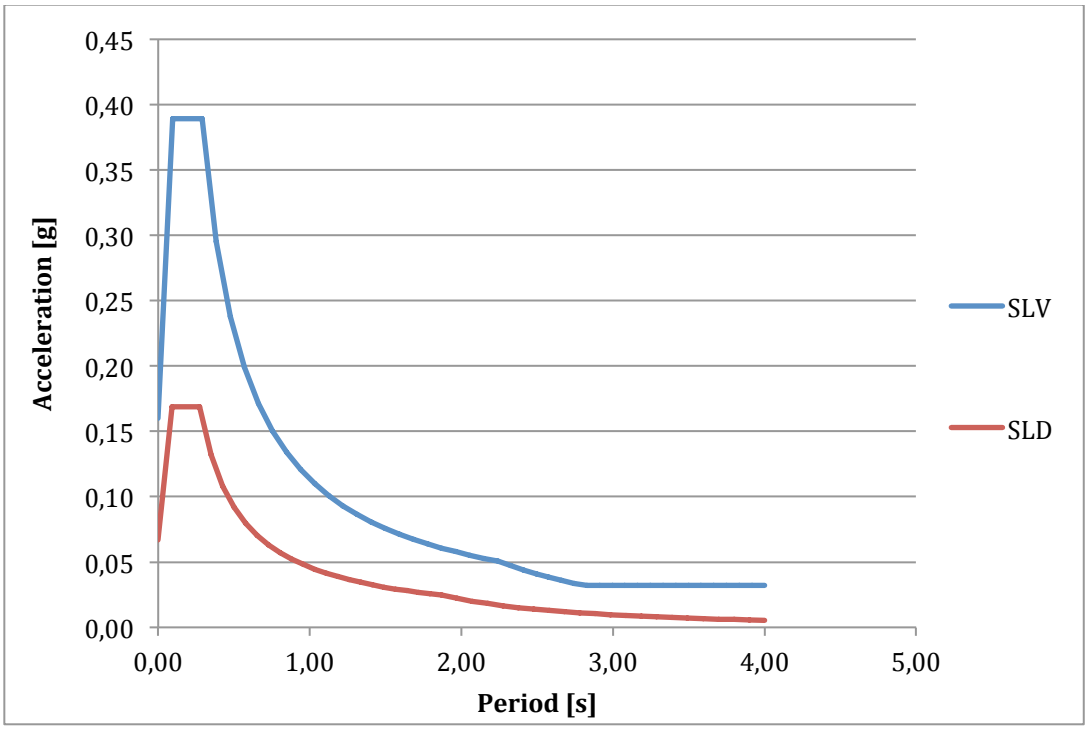

Picture 54. Elastic design spectra

STATO LIMITE	SLV
a_g	0,160 g
F_o	2,431
T_C	0,292 s
S_S	1,000
C_C	1,000
S_T	1,000
q	2,400

Table 8. Parameters for SLV

STATO LIMITE	SLV
a_g	0,160 g
F_o	2,431
T_C	0,292 s
S_S	1,000
C_C	1,000
S_T	1,000
q	1,000

Table 9. Parameters for SLD

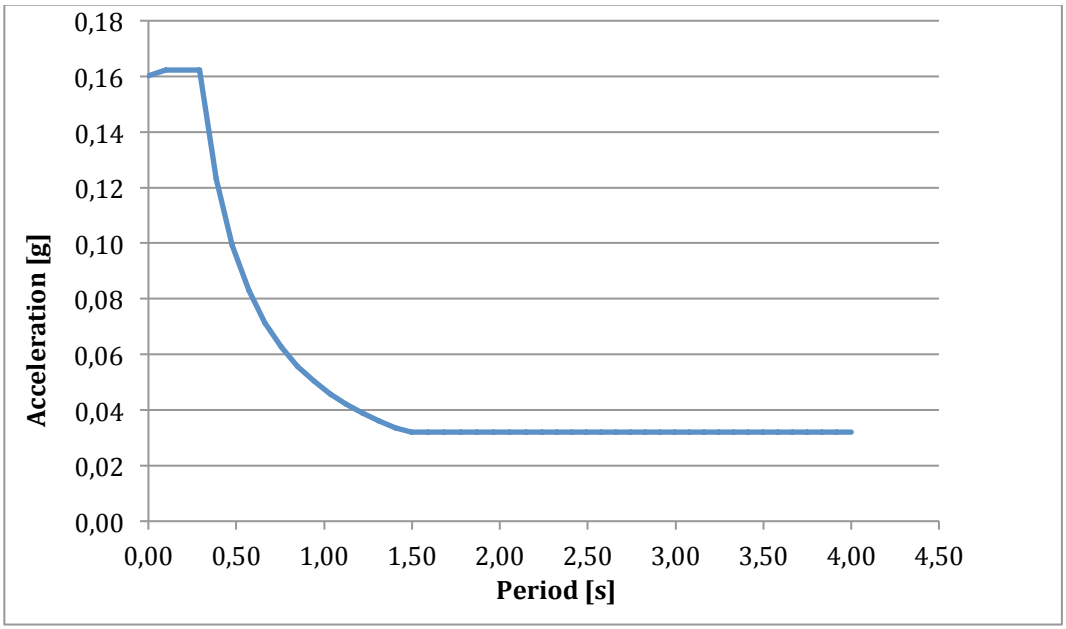

Picture 55. Inelastic design spectrum (SLV)

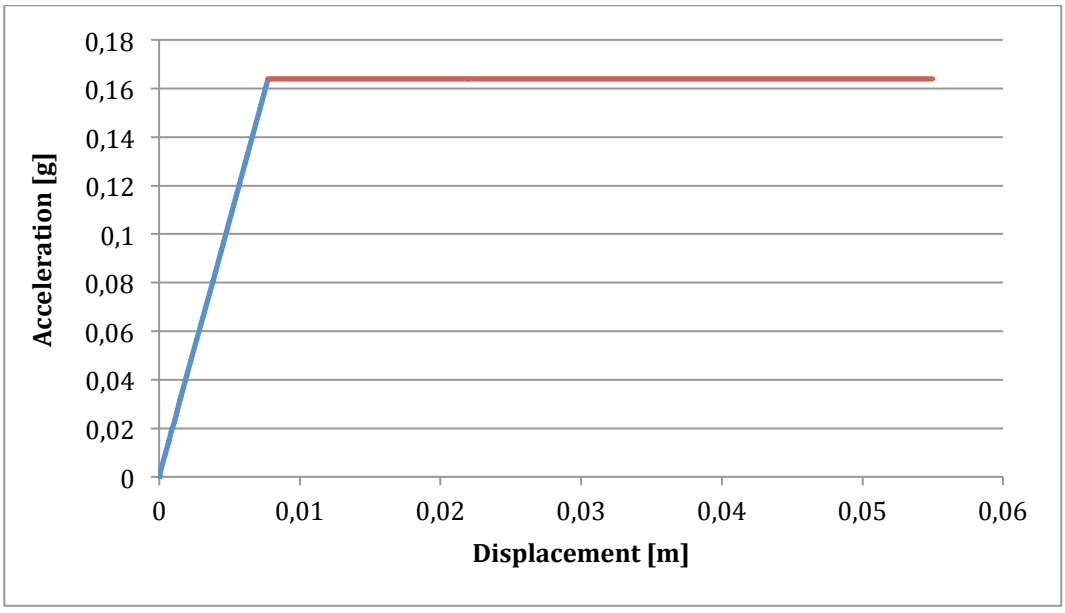

Picture 56. Front wall acceleration-displacement capacity curve

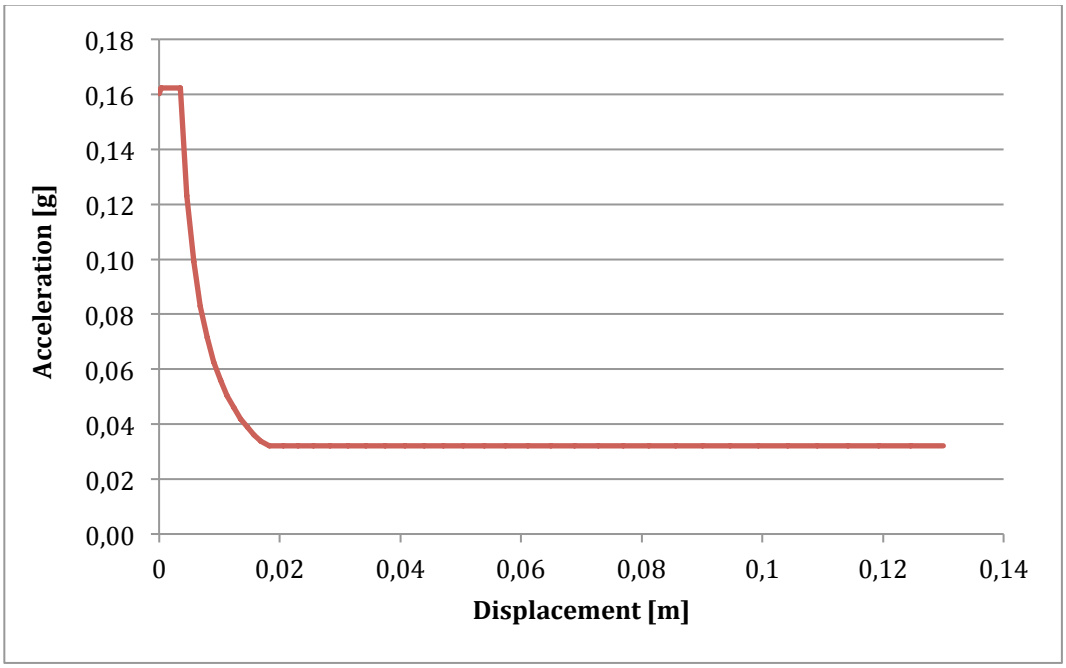

Picture 57. ADSR inelastic design spectrum (SLV)

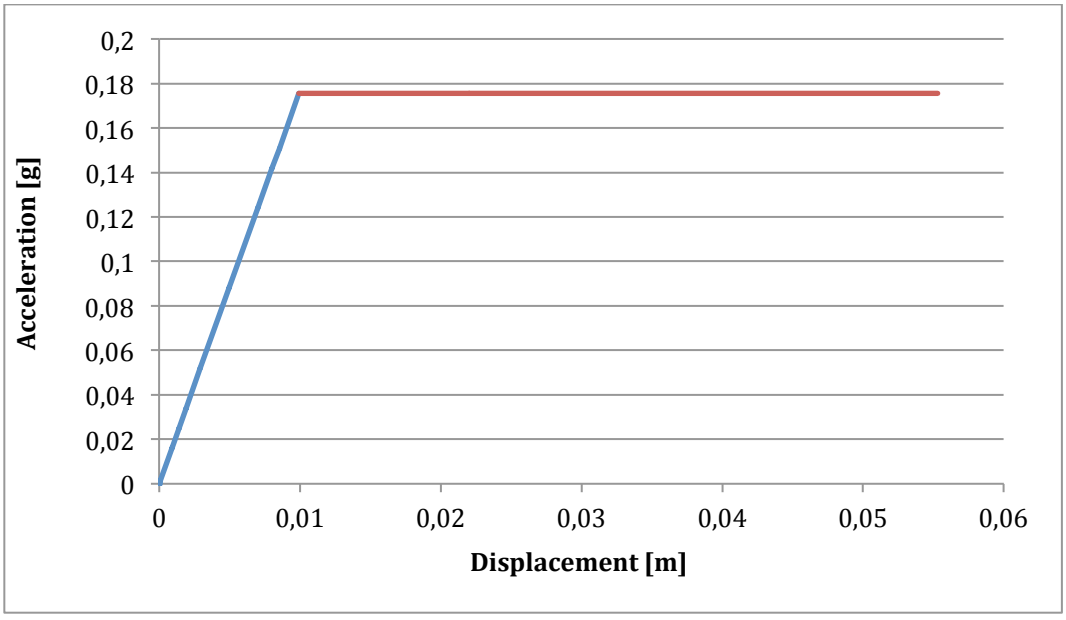

Picture 58. Right handside wall acceleration-displacement capacity curve

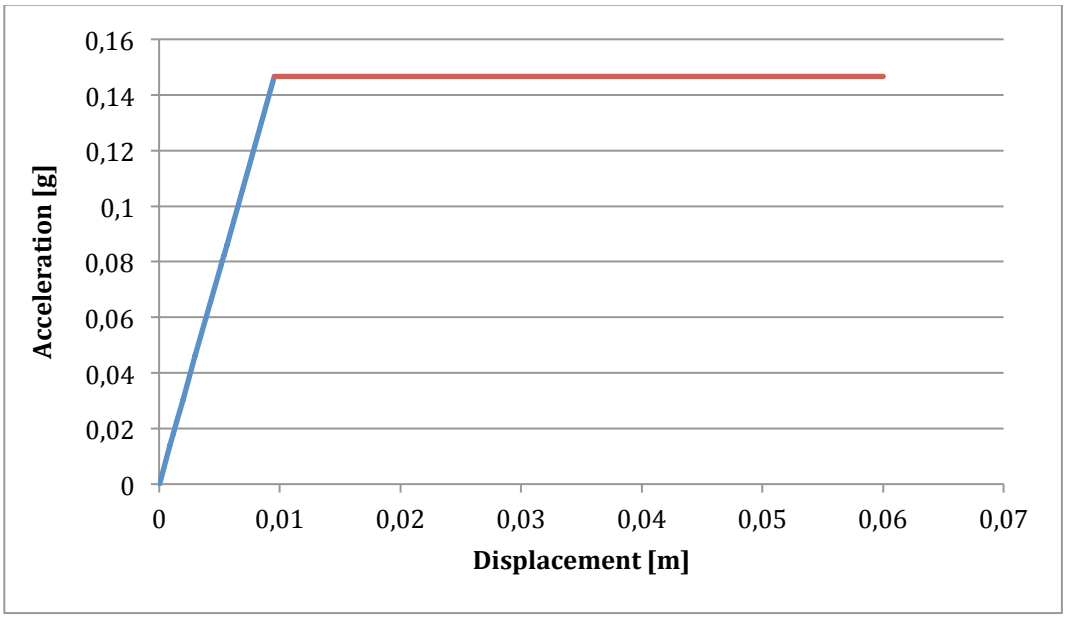

Picture 59. Left handside wall acceleration-displacement capacity curve

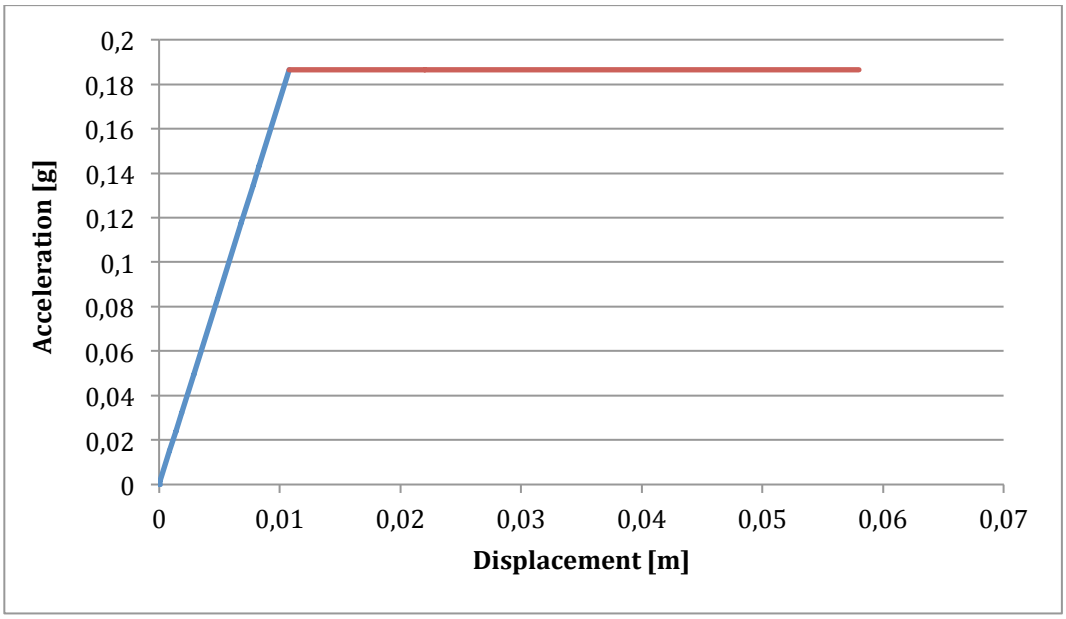

Picture 60. Back wall acceleration-displacement capacity curve

Chapter 7

Analysis of results and seismic assessment

7.1 General approach

Once we come to the verification of results, first of all a superposition between the capacity curve and the relative limit state's design spectrum is needed in order to evaluate the *performance point*.
After that, following the recommendations of NTC08, precise verifications are carried out according to the type of considered limit state; in particular, §§7.3.6.2 for SLV and 7.3.7.2 for SLD allow to select specific assessment criteria in terms of deformation and displacement.

7.2 SLV Verification

The superposition of capacity curve and seismic spectra (see, as a reference, picture 61) reveals that the behaviour of the walls stands elastic even beyond the inelastic demand: in this case, we need to use the elastic spectrum as the design one and reduce it according to the ductility μ evaluated as the ratio between the *demand ultimate displacement* and yielding displacement. In particular, the first one is obtained by the prolongation of the elastic trend until the elastic spectrum is reached: the correspondent value of displacement is the demand ultimate displacement. For a better understanding see picture 62.

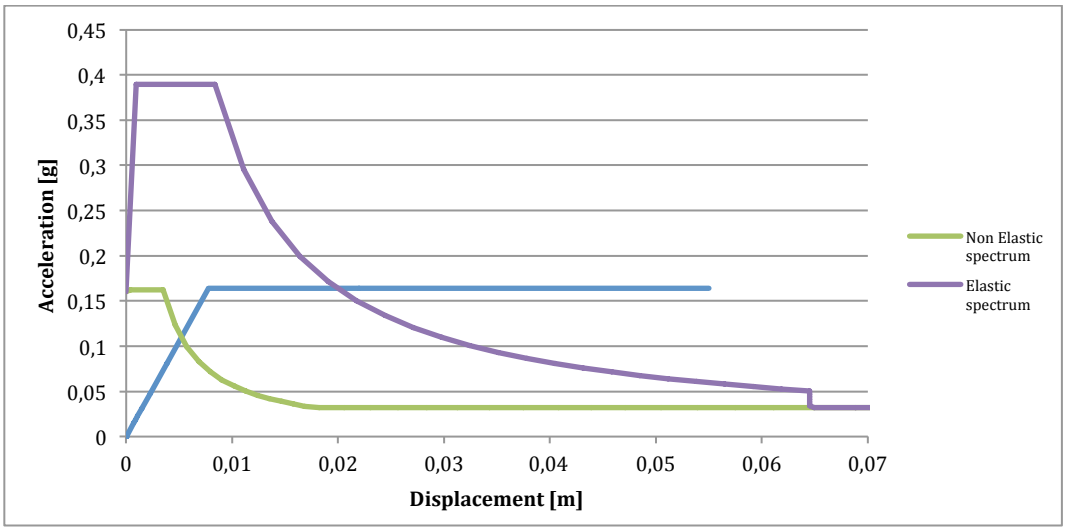

Picture 61. Superposition for SLV – Front wall

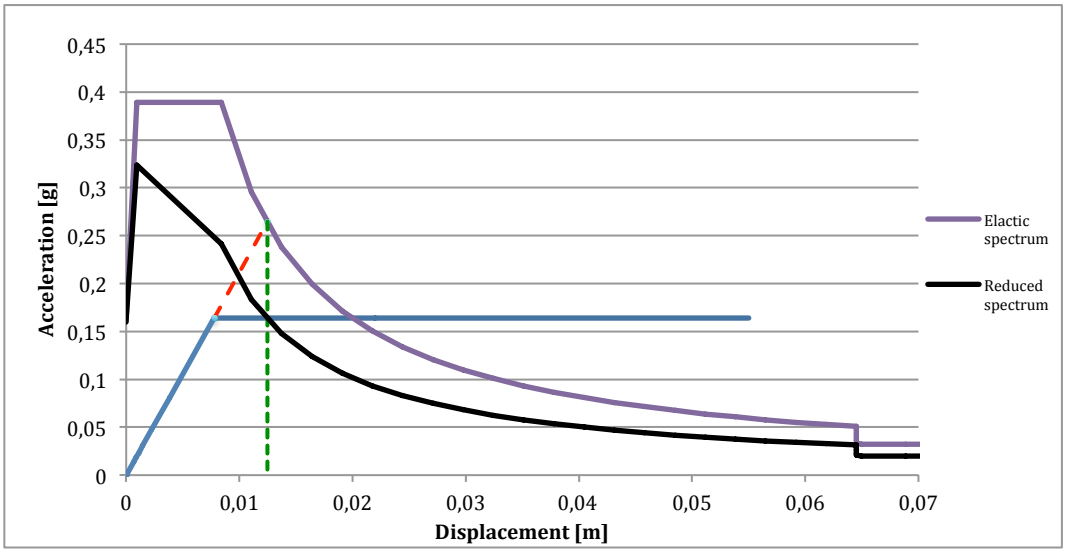

Picture 62. Reduction of inelastic spectrum for SLV – Front wall

The value for μ is, then, 1,61 so that, recalling the relations to be used to compute R_μ(μ,T) (5.3 and 5.4) as a function of T_C = 0,291s, the new design spectrum is obtained as:

$$S_A(T,\mu) = \frac{S_e(T)}{R_\mu(\mu,T)} \quad (7.1)$$

The black line in picture 62 represents the result of this reduction; as we can see, the inelastic demand in terms of acceleration is the one related to the intersection point between capacity curve and demand spectrum with ductility μ: at this point the ductility factor determined from the capacity curve is equal to the one associated with the intersecting demand spectrum.
Finally, we have to simply verify whether the displacement capacity is greater than the displacement demand or not, according to NTC08 §§7.3.6.2: this is nothing but making a comparison between the ultimate displacement given by the pushover analysis and the demand ultimate displacement obtained by the previous graphical method; the results for the four walls are collected in table 10, while pictures 63, 64 and 65 display the reduction of the correspondent inelastic spectra for the missing walls.

	Ultimate displacement [m]	Demand ultimate displacement [m]
Front Wall	0,050	0,013
Right Handside Wall	0,055	0,014
Left Handside Wall	0,060	0,015
Back Wall	0,058	0,014

Table 10. Displacement verification SLV

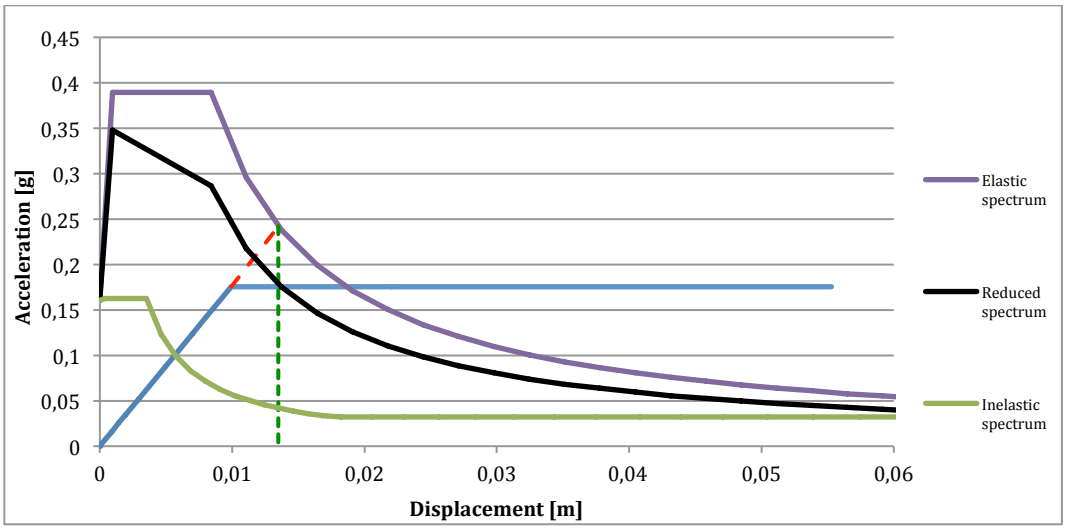

Picture 63. Reduction of inelastic spectrum for SLV – Right handside wall

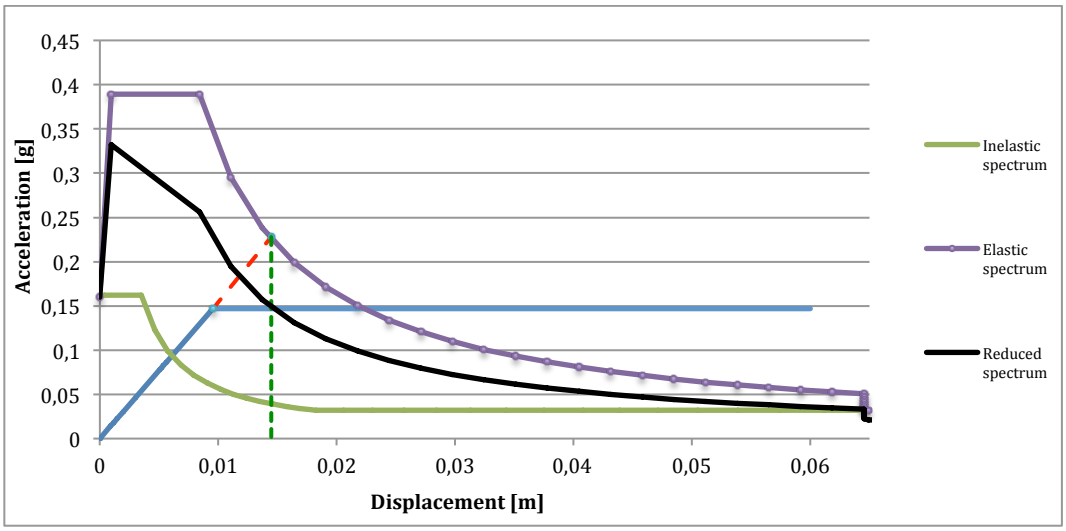

Picture 64. Reduction of inelastic spectrum for SLV – Left handside wall

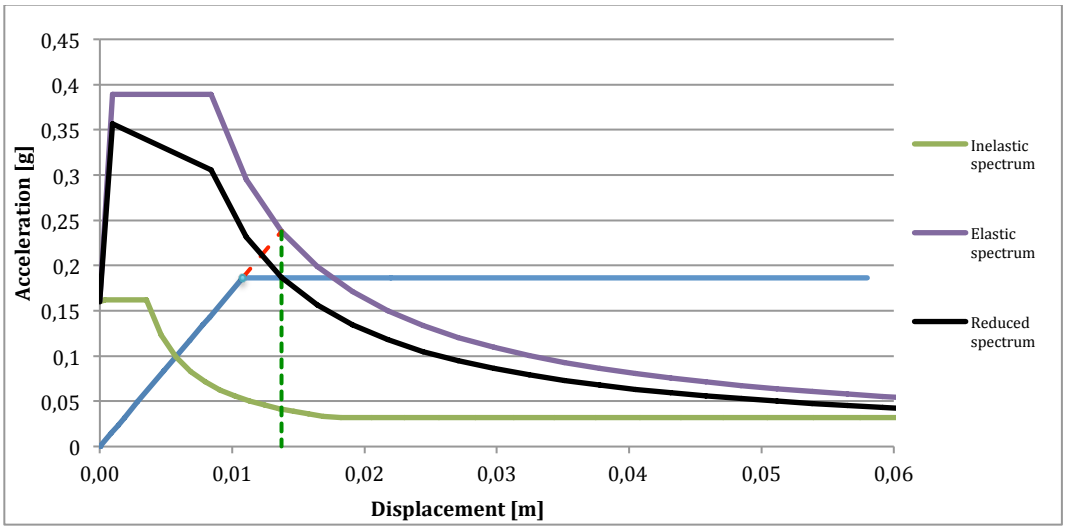

Picture 65. Reduction of inelastic spectrum for SLV – Back wall

All the previous results show that the walls provide a high resistance to the design seismic event, being able to reach displacement that are, on average, three times greater than the demand value. Moreover, we can notice there is not any particular difference among the resulting numbers showing a quite homogeneous behaviour of the external structure of the building.

7.3 SLD Verification

As well as for the SLV case, the superposition of the design spectrum and capacity curve allows a complete comparison between the demand and the resistance of the structural element; following the NTC08 §§7.3.7.2, for serviceability limit state the elastic spectrum is to be considered.

Once we qualitatively verify the resistance of the wall, a further verification can be performed from a numerical point of view; more precisely, we need to evaluate the relative displacements d_r between floors and check whether:

$$d_r < 0,003h \quad (7.2)$$

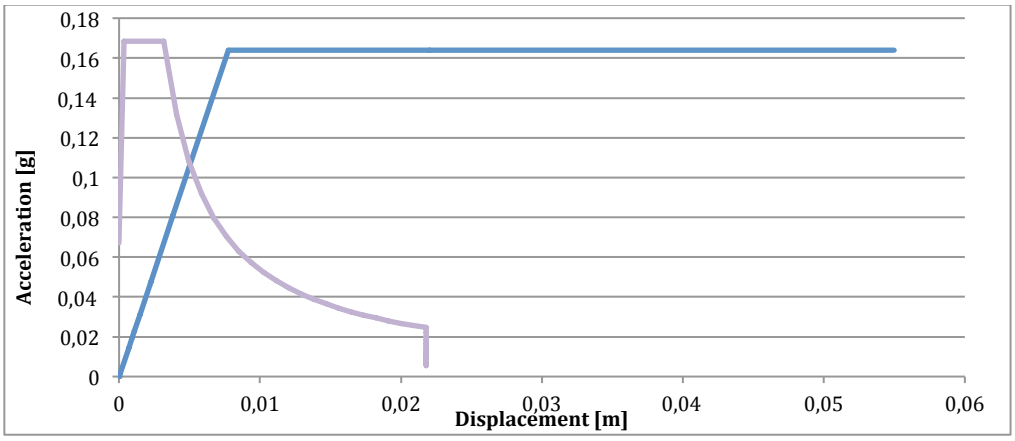

Picture 66. Superposition for SLD – Front wall

The previous relation is valid for structural masonry, with *h* as the height of each floor. Table 11 collects the results for the four walls. Besides, pictures 67, 68 and 69 show the graphical superposition for the remaining walls.

	dr1 [m]	dr2 [m]	dr3 [m]	0,003h1 [m]	0,003h2 [m]	0,003h3 [m]
Front Wall	0,0016	0,0010	0,0003	0,012	0,026	0,035
Right Handside Wall	0,0016	0,0021	0,0004	0,012	0,026	0,035
Left Handside Wall	0,0015	0,0020	0,0011	0,010	0,024	0,032
Back Wall	0,0014	0,0015	0,0006	0,013	0,025	0,035

Table 11. Displacement verification SLD

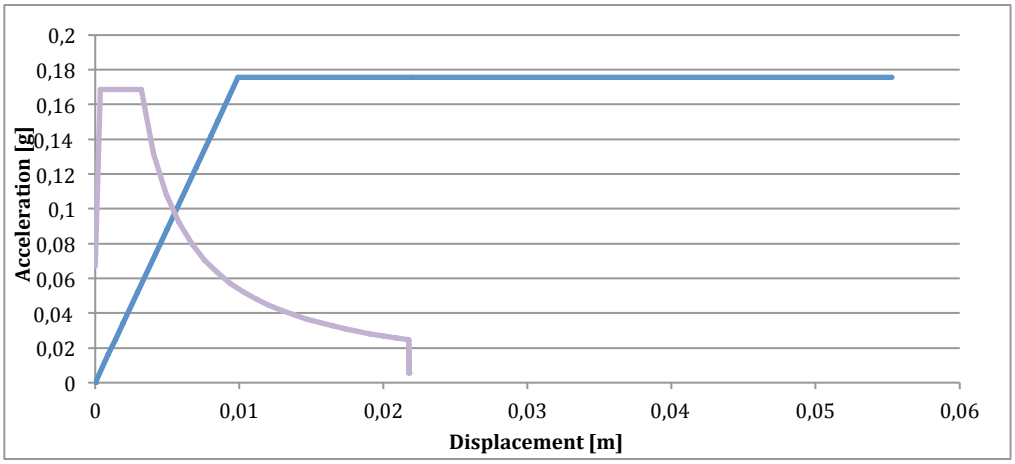

Picture 67. Superposition for SLD – Right handside wall

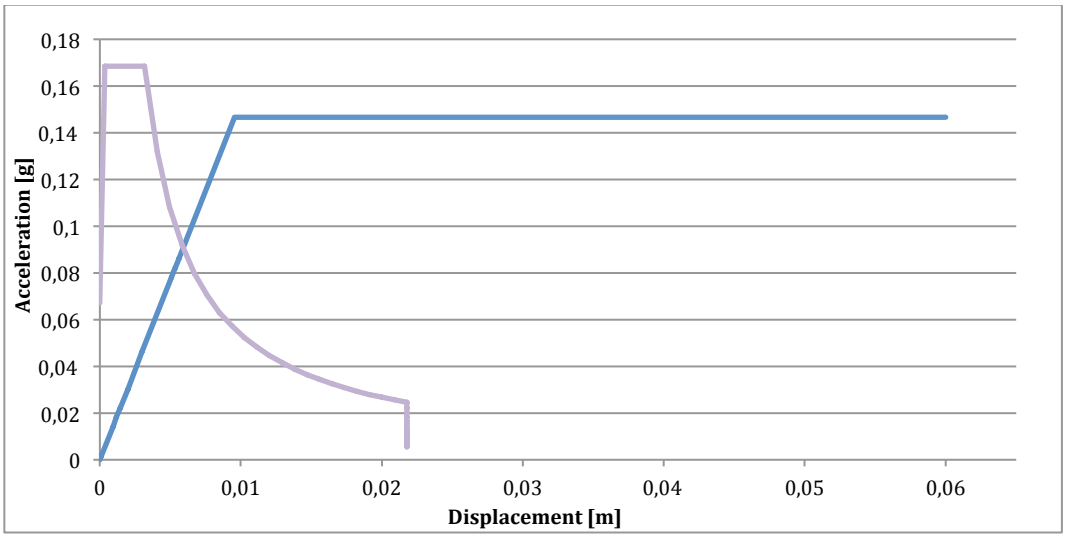

Picture 68. Superposition for SLD – Left handside wall

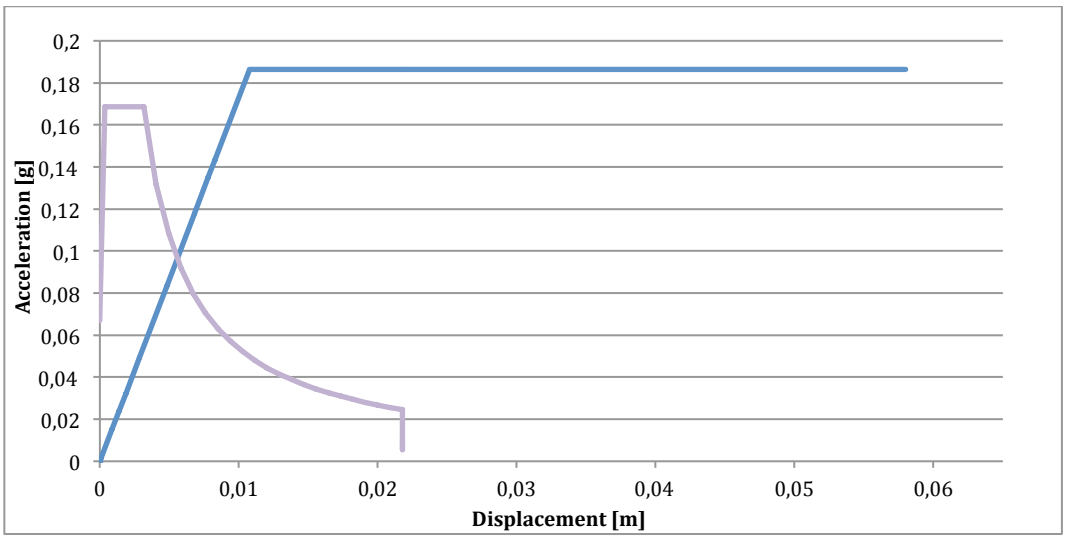

Picture 69. Superposition for SLD – Back wall

According to the previous results, the assessment of the seismic resistance of the four walls is, once again, highly positive: all of them show an elastic behaviour which goes greatly beyond the elastic limit set by the demand spectrum. Moreover, the relative displacements are really small with respect to the bound given by regulations, representing a compact global deformation of the walls.

Chapter 8

Retrofit solution for slabs and vaults

8.1 General considerations

As shown in Chapter 7, the case study reveals a great seismic resistance given by high ductility and capability of non-linear deformation; in this situation, we could try to generally improve the structural characteristics of the building, providing updates of elements that are particularly old or damaged as well as enhancing safe components that lack of certain practical details.
In particular, once the primary investigation has been done, two of the main structural peculiarities that have been pointed out are: the presence of vaults and two order timber beams slabs as the most likely (see Chapter 1). Both of them have been commonly used in historical buildings and, after a long time, they could suffer from the effect of their age; besides, a stiffening retrofit can be necessary, and generally advisable, especially for timber slabs, whose natural features may result in a too elastic response and deformation.
According to all the previous, this chapter aims at explaining two of the major slabs and vaults' retrofitting techniques that are considered suitable for the current case study.

8.2 Slabs retrofitting

Old timber slabs often require strengthening works since, being dimensioned for low accidental loads, they lack of structural resistance, which might be caused even by a change in the usage of the building: for instance, we can refer to the numerous historical edifices that have been recently turned into public offices or libraries or schools. Moreover, the functionality of such slabs could be frequently compromised by the excessive deformation happened in the past, involving even non-structural elements.

Generally, timber structures are substituted by brand new slabs since they are highly exposed to natural decay, but, sometimes, a rehabilitation work seems more convenient or even necessary (according to prescriptive restrictions); in this situation, the estimate of the preservation condition of timber is fundamental in order to assess whether a rehabilitation can be actually performed or not: at this stage, it is necessary to clearly know that no biological decay is present so that timber is still properly working.

As far as the case study is concerned, we deal with timber-brick slabs: they can be seen as standard timber slabs where a brick made planking is arranged over the timber frame; besides, they are all well preserved without showing any particular external decay proof. (see Chapter 1 pictures 5, 6 and 7).

In this situation, the best type of strengthening could be pouring a thin concrete sheet linked to the primary timber beams by means of connectors: the latters are particularly useful to solve the majority of rehabilitation problems; moreover, the static scheme they provide allows to exploit the best performances of both materials. In fact, the interposition of such connectors controls the relative slipping and creates a new section where, due to vertical actions, wood is under traction, while concrete is compressed.

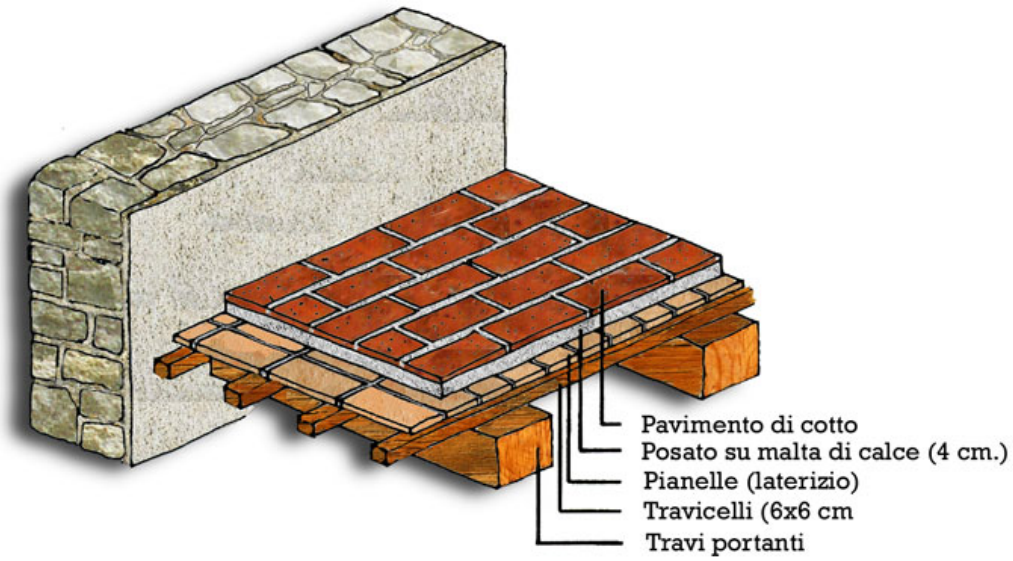

Picture 70. Timber-brick slab

The resulting mixed structure is, eventually, able to outstandingly employ the peculiarities of the two materials, thus increasing the slab capacity in terms of resistance and stiffness.

The main reason why this operation is, here, suggested is due to the fact that, when performing the FEM simulation, a concrete beam has been assumed in order to represent the presence of a rigid slab (see Chapter x): the quality of outcomes of the seismic verification has, in fact, advised that the existence of rigid slab can result in a safer overall condition for the building.

Furthermore, the major advantages of this practice are:

- Increase in slab's stiffness: we can get up to 10 times the initial stiffness thanks to the elastic modulus of concrete
- Increase in load capacity
- Vibration control
- Improving acoustic comfort
- Enabling the addition of a insulators

- Fire resistance
- Simplifying the linkage between slab and masonry in order to realize curbstones: in fact, the timber frame cannot be considered as a rigid connection capable of transmitting horizontal seismic forces.

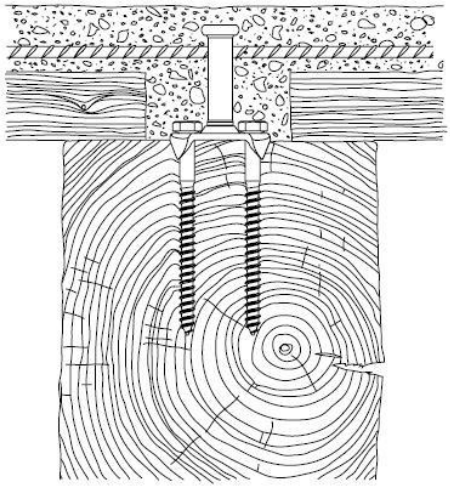

Picture 71. Reinforced timber beam

In order to get a correct and functioning usage of the connectors, it is fundamental to follow precise instructions; first of all we need to take out the materials (pavement and any other loose element) over the wood frame so that a full and accurate cleaning can be done. At the same time, we have to check if any decay is present and, in case, provide a substitution where possible.

Once the surface has been polished, connectors have to be fixed to principal beams; they need to be correctly dimensioned according to loads and slab's width. Besides, the connectors should be alternated so that we do not insist over the same portion of timber.

It is, then, generally suggested to put a transpiring waterproof barrier in order to avoid water percolation and dust formation; moreover the slab is

shored up before pouring the concrete and it is kept supported until the concrete reaches a complete maturation.
Finally, an electrowelded net is to be placed within the concrete slab in order to absorb the tensile stresses.

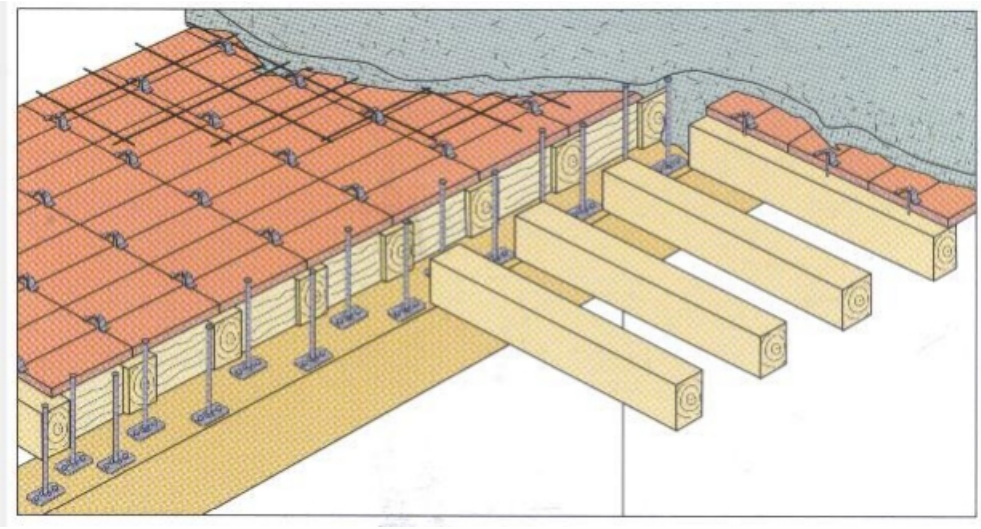

Picture 72. A reinforced timber slab

8.3 Vaults retrofitting

When dealing with vaults, there are many different kinds of retrofit we can perform according to the field in which we want to act; for example, we can have:

- Reduction of the loads on the vault (especially for seismic situation) by means of removal of heavy and incoherent filling and substituting them with lightweight concrete spandrels
- Limiting the deformations of the extrados by means of spandrels or dwarf walls
- Increasing the vault's thickness with a cloak of reinforced concrete properly linked to the vault itself

- Inserting tie-rod, which avoid the displacement of boundary walls

As far as the analysed case is concerned, the suggested method consists in the creation of a reinforced concrete "counter-vault" located at the extrados; this procedure is quite common for historical arches and vaults and basically involves linking between the existing vault and the counter-vault: it seems as if a sort of new thicker vault is cooperating with the underlying one from a resistance point of view. However, the difference in stiffness makes the RC cloak to bear a higher percentage of accidental load acting on the structure.
The main advantages of this practice are:

- Ability of the extrados to absorb even traction stresses thanks to the presence of the steel reinforcement of the cloak
- The binding action provided by coupling between masonry and concrete

On the other hand, the main drawbacks of such method are:

- Inability of reaching the extrados once the cloak is placed so that no future inspections can be done
- Great increase in self weights
- Likely negative interaction between masonry and concrete (water percolation, salt filtration, ecc.)

Nowadays, very thin RC concrete cloaks (4-8cm) are realized in order to reduce their stiffness and weight: in fact, an excessive rigidity could lead to a discharge of the vault and a high overburden could turn the load situation upside down.

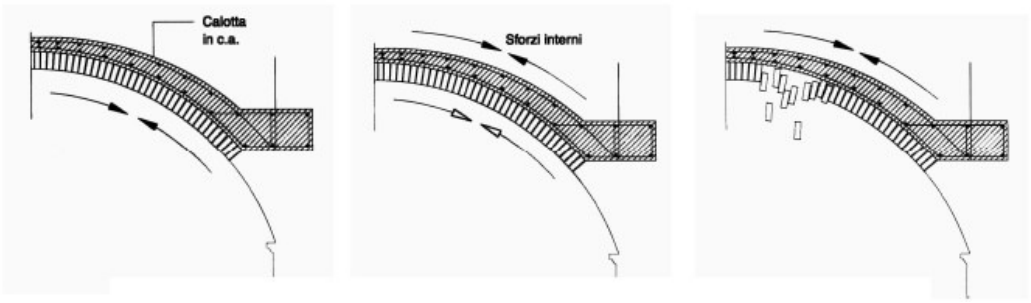

Picture 73. Consequence of excessive rigidity of the cloak

The main phases of construction are then:

- *Shoring up*: it is needed to hold up the supporting structure (*centina*), which, in turn, supports the vaults
- *Removal of pavements and spandrels*: after the pavements have been taken away, the spandrel is removed by hand avoiding any use of vibrating tool; this removal must be performed as much uniformly as possible since, in this way, negative effects due to asymmetric elimination of materials are prevented. Once the procedure is finished, the extrados is carefully polished by blowing (*soffiatura*) and washing.
- *Cloak's realization*: holes (36 mm) are created in the perimetral walls with no more than 50 cm spacing, and then reinforced with steel rods (10-12 mm) anchored by means of epossidic resin. After that, the electrowelded net is placed with maximum diameter of 6 mm for 10x10 cm mails. The net is linked to the perimetral walls' connections by welding and rolled out over a resin layer. Eventually, the concrete is poured for a 4-5 cm thickness.
- *Spandrels' pouring*: the spandrels are restored once the concrete has hardened: they can be made of expanded clay.

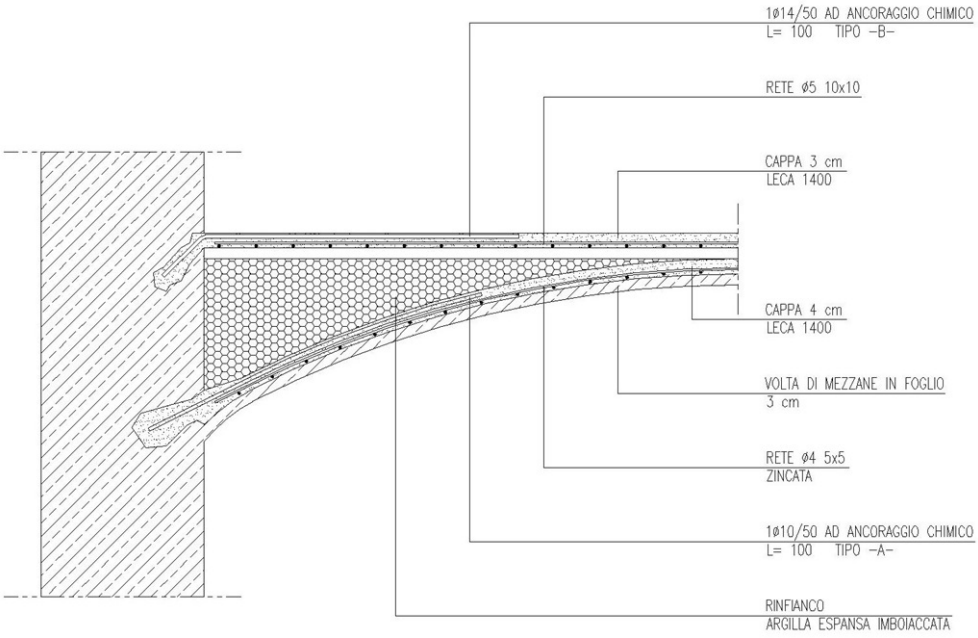

Picture 74. Example of strengthening work

Moreover, when dealing with seismic force, we cannot rely only on friction-based mechanisms so that additional intervention can be used; the most common practice is the application of tie-rods.

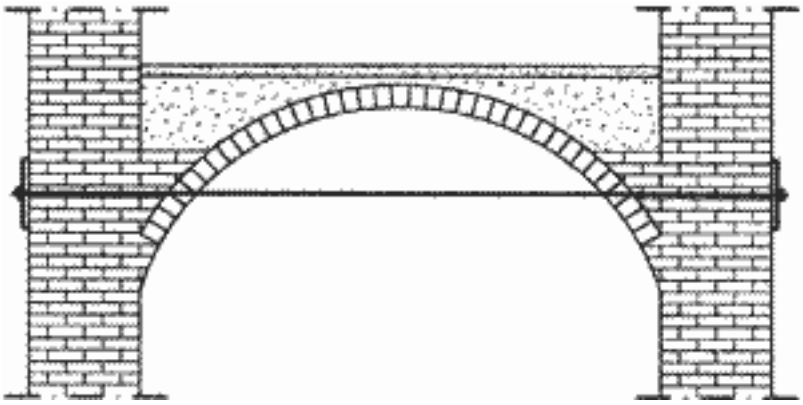

Picture 75. Example of tie-rod disposition

However, as far as the case study is concerned, the latter seems an excessive precaution given the quality of the seismic response of the structure.

Conclusions

The developed work has been a well organized and harmonic sequence of actions, whose result is, basically, only one: a clear and wide knowledge of the analysed building under many kind of aspects; by means of this study, plenty of information have been collected: some of them are new ones and some other are simply re-discovered. Anyway, we can surely say that every single material used has given its contribution to the final goal, making the overall understanding a bit easier.

The importance of the edifice, given by its long history, requires a detailed analysis in order to ensure its safety towards a longer preservation: in this context, the detailed metrical evaluations as well as the primary investigation allow the identification of the static scheme.

Eventually, the results of the seismic assessment are more than satisfactory, showing all the four walls are actually capable of reaching a high ductility.

Notwithstanding the positive performance of the structure, it is important to regularly check its state in order to prevent any possible worsening: in this sense, this dissertation would provide many useful resources for further rehabilitation and strengthening works. Besides, the updates of aged information that has been initially exposed assume a fundamental importance as well as being a long-lasting valuable asset.

Bibliography

Historical sources

Albergotti A., *Istoria della famiglia Albergotti descritta da E. Gamurrini*, 1688.

AA.VV, *I capitol del Comune di Firenze*, Firenze, 1886.

A.S.A., *Catasto antico di Città: Porta S. Spirito* (da c. 490 a c. 498).

A.S.A., *Catasto antico di Città: Porta S. Lorentino* (ac. 103).

A.S.A., *Catasto Lorenese: Voltura 1783* (ac. 53).

A.S.A., *Catasto Napoleonico: Voltura 1807 Tomo II* (ac.748).

A.S.A., *Catasto Napoleonico: Voltura 1808* (ac. 570-571).

Benigni P., Carbone L., Saviotti C., *Gli albergotti: famiglia, memoria, storia: atti delle giornate di studio, Arezzo 25-26 novembre 2004,* EDIFIR, Firenze 2006.

Carapelli G, *Scheda T.P.Beni A.A. n° cat. 09/00237066*, Sop. S.A.A.A.S. di Arezzo.

Massetani F.A., *Dizionario bibliografico degli aretini ricordevoli nelle lettere, scienze, arti, armi e religione*, Biblioteca Città di Arezzo, Arezzo, 1942.

Paganelli M., *Modelli reticolari per l'analisi pushover di strutture murarie*, Tesi di laurea, Univ. di Bologna, Facoltà d'Ingegneria, 2007.

Pompa N., *Analisi sismica di telai in C.C.A. con tamponamenti*, Tesi di Laurea, Univ. di Bologna, Facoltà d'Ingegneria, 2012.

Tafi A., *Immagine di Arezzo – La città oltre le mura medicee e il territorio comunale*, Cortona, 1985.

Tafi A., *I vescovi d'Arezzo*, Cortona, 1986.

Publications

"Analisi static non lineare (Pushover)", Albanesi T., Nuti C., Dipartimento di Strutture, Roma, 2007.

"Analisi strutturale degli edifice in muratura secondo la nuova normativa sismica: guida all'applicazione di un Software dedicato", Convegno, Aedes Software, Ancona 4 aprile 2007.

"Progettazione di strutture in muratura in zona sismica", Prof. Ing. Benedetti A., Dip. DICAM, Univ. di Bologna.

"A Nonlinear Analysis Method for Performance Based Seismic Design", Fajfar P., Eeri M., Earthquake Spectra, Vol. 16, No 3, pp. 573-592, August 2000.

Textbooks

Augenti N., *Il calcolo sismico degli edifice in muratura*, Nuova edizione, 2004.

Calcea L., De Vecchi A., *Tecnologie di consolidamento delle strutture murarie*, D. Flaccovio, 1990.

Tomaselli L., *L'edificio antisismico in muratura*, presentazione di Sergio Lagomarsino, Vitali e Ghiandai, Genova, 2000.

Regulations

Decreto 20 novembre 1987, *Norme tecniche per la progettazione, esecuzione e collaudo degli edifice in muratura e per il loro consolidamento.*

Eurocodice 6, *Progettazione delle strutture in muratura – Parte 1-1 regole generali per gli edifice – Regole per la muratura armata e non armata*, UNI ENV 1996-1-1.

Ordinanza 3431 – Testo integrato dell'allegato 2 – Edifici – all'ordinanza 3274 come modificato dall'OPCM 3431 del 3/5/05. *Norme tecniche per il progetto, la valutazione e l'adeguamento sismico degli edifici.*

Decreto ministeriale 14 gennaio 2008 – NTC2008

Manuals

Theoretical background to the Straus7 finite element analysis system, Theoretical Manual.

SismiCadUndici: Tutor SismiCad 11.10 – Pushover Muratura, Manuale tecnico.

Ringraziamenti

L’importanza e il significato di questa tesi vanno oltre il rappresentare la fine di un percorso che, purtroppo, è giunto al termine.
Molte persone intorno a me la ricorderanno nei modi più diversi, avendo vissuto aspetti complementari del suo sviluppo.
Ringrazio, quindi, ognuno di loro e, in modo particolare, il Prof. Andrea Benedetti, i Marchesi Albergotti e tutti coloro che hanno camminato al mio fianco.

Attachments

A.1

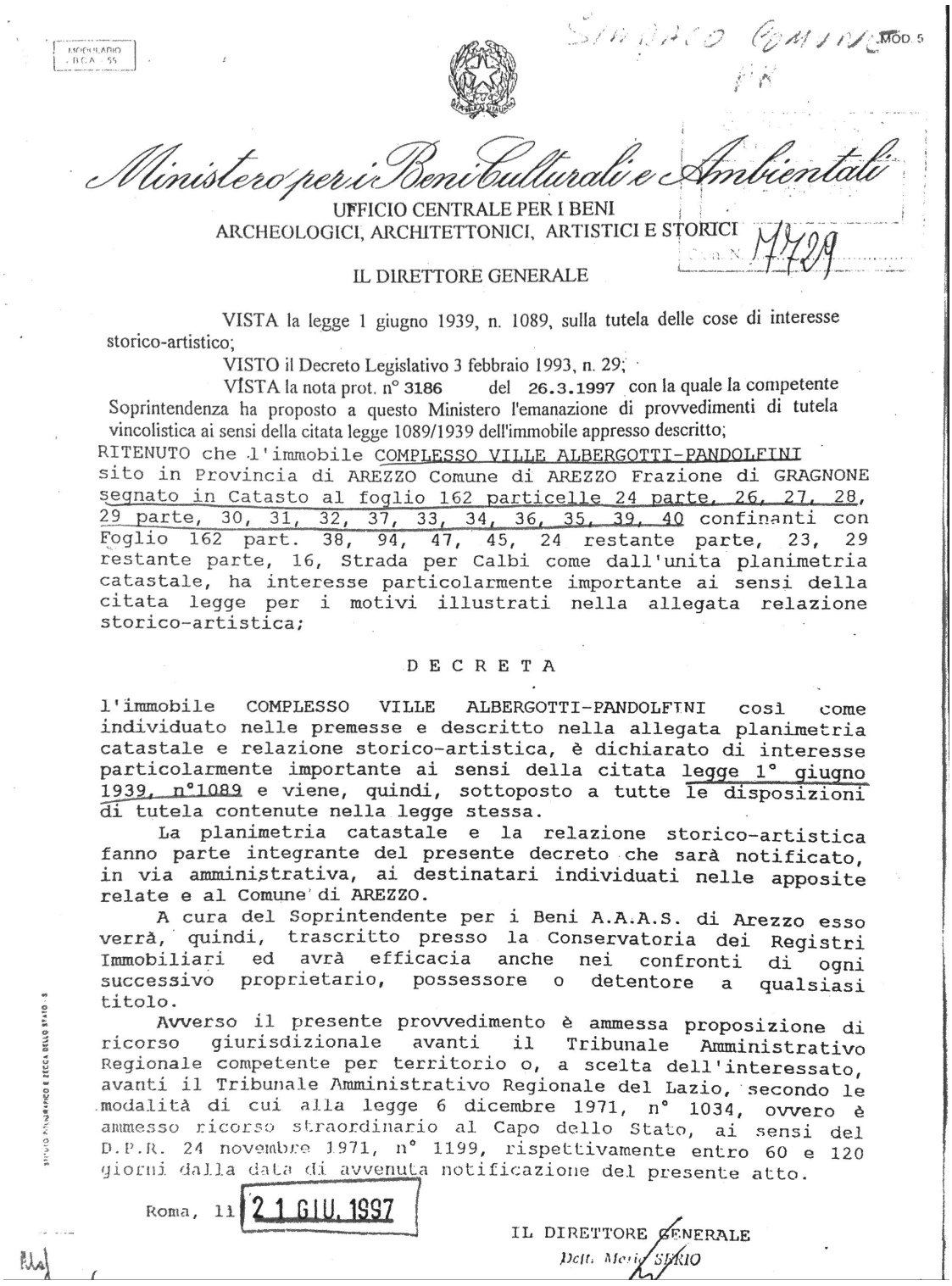

MODULARIO F.B.C.A. - 55

MOD. 5

Sindaco Comune

Ministero per i Beni Culturali e Ambientali

UFFICIO CENTRALE PER I BENI
ARCHEOLOGICI, ARCHITETTONICI, ARTISTICI E STORICI

Div. N. 17429

IL DIRETTORE GENERALE

VISTA la legge 1 giugno 1939, n. 1089, sulla tutela delle cose di interesse storico-artistico;

VISTO il Decreto Legislativo 3 febbraio 1993, n. 29;

VISTA la nota prot. n° 3186 del 26.3.1997 con la quale la competente Soprintendenza ha proposto a questo Ministero l'emanazione di provvedimenti di tutela vincolistica ai sensi della citata legge 1089/1939 dell'immobile appresso descritto;

RITENUTO che l'immobile COMPLESSO VILLE ALBERGOTTI-PANDOLFINI sito in Provincia di AREZZO Comune di AREZZO Frazione di GRAGNONE segnato in Catasto al foglio 162 particelle 24 parte, 26, 27, 28, 29 parte, 30, 31, 32, 37, 33, 34, 36, 35, 39, 40 confinanti con Foglio 162 part. 38, 94, 47, 45, 24 restante parte, 23, 29 restante parte, 16, Strada per Calbi come dall'unita planimetria catastale, ha interesse particolarmente importante ai sensi della citata legge per i motivi illustrati nella allegata relazione storico-artistica;

D E C R E T A

l'immobile COMPLESSO VILLE ALBERGOTTI-PANDOLFINI così come individuato nelle premesse e descritto nella allegata planimetria catastale e relazione storico-artistica, è dichiarato di interesse particolarmente importante ai sensi della citata legge 1° giugno 1939, n°1089 e viene, quindi, sottoposto a tutte le disposizioni di tutela contenute nella legge stessa.

La planimetria catastale e la relazione storico-artistica fanno parte integrante del presente decreto che sarà notificato, in via amministrativa, ai destinatari individuati nelle apposite relate e al Comune di AREZZO.

A cura del Soprintendente per i Beni A.A.A.S. di Arezzo esso verrà, quindi, trascritto presso la Conservatoria dei Registri Immobiliari ed avrà efficacia anche nei confronti di ogni successivo proprietario, possessore o detentore a qualsiasi titolo.

Avverso il presente provvedimento è ammessa proposizione di ricorso giurisdizionale avanti il Tribunale Amministrativo Regionale competente per territorio o, a scelta dell'interessato, avanti il Tribunale Amministrativo Regionale del Lazio, secondo le modalità di cui alla legge 6 dicembre 1971, n° 1034, ovvero è ammesso ricorso straordinario al Capo dello Stato, ai sensi del D.P.R. 24 novembre 1971, n° 1199, rispettivamente entro 60 e 120 giorni dalla data di avvenuta notificazione del presente atto.

Roma, li 21 GIU. 1997

IL DIRETTORE GENERALE
Dott. Mario SERIO

A.2

MODULARIO
B.C. - 3

MOD. 7

Ministero per i Beni Culturali e Ambientali

SOPRINTENDENZA PER I BENI A.A.A.S. DI AREZZO

AREZZO - Loc. Gragnone - Complesso Ville Albergotti-Pandolfini

RELAZIONE STORICO-ARTISTICA

A poca distanza da Arezzo, nella frazione di Gragnone, lungo la riva del torrente Vingone, spicca la notevole mole del complesso di Villa Albergotti-Pandolfini.
L'agglomerato edilizio formatosi nell'arco dei secoli XVII-XIX ingloba un antico fortilizio del XIII-XIV° Sec. già di proprietà degli Albergotti, posto a difesa della valle del Bagnoro e di Arezzo.
Più volte ampliato e trasformato in villa con annessa fattoria, il complesso fu per ragioni di eredità, ulteriormente diviso ed ampliato a partire dalla seconda metà del XVIII° Secolo, allorché parte della villa passò ai Pandolfini.
Potente famiglia di origine germanica, il casato degli Albergotti risulta iscritto fra i patrizi aretini "ab immemorabili".
L'Abate Gamurrini, ne parla come "...avanzo dei regi toscani, venuti come gli Ubertini ed i Barbolani, dagli Attaberti, stipite ne fu un certo Teobaldo che fiorì nell'890... nella seconda metà del XIII° Secolo Raimondino Albergotti, cavaliere a seguito dell'Imperatore Corradino di Svevia, fermatosi a Firenze, generò la famiglia degli Albizi, come si legge in "Storie fiorentine" di Scipione Ammirato; mentre da Bernardo di Raineiro, nel 1000, vennero i Cattani di Diacceto...". Nel 1350, gli Albergotti furono iscritti alla nobiltà fiorentina, come guelfa, nella persona del legale Francesco di Bico Albergotti. "Nella linea di priore hanno dal 1613 il titolo di Baroni per antico diploma del re di Polonia Casimiro III, confermato dal Granduca Cosimo III con decreto 1756... La linea d'Albergotto d'Angelo Tommaso, acquistò il marchesato di Polino nel 1761 coi privilegi che godeva la famiglia Castelli di Terni, per concessione di Papa Gregorio XIII". (Massetani)
L'arme: in campo d'oro tre bande nere oblique con stelle d'oro nella banda centrale.

Parzialmente visibili dal chiostro che divide le due attuali proprietà, i ruderi del medioevale fortilizio ed il mastio, denunciano le prime facies del complesso. Sottomesso ai Fiorentini nel marzo del 1384, il forte perse nei secoli, la sua funzione difensiva, finché nella seconda metà del XVI° Sec. diventa "casa da padrone e da lavoratori" di proprietà di Nerozzo Albergotti.
Alla fine del Cinquecento, il complesso fu ereditato dal Cav. Girolamo di Nerozzo che lo lascia nel 1636 ai figli Albizo e Cosimo. Ed è proprio a quest'ultimo che si deve il primo vero assetto della villa e della Cappella, dedicata a S.Cristina (1648)
Ecclesiastico, nonché paggio e cameriere del Cardinale Carlo de Medici, Cosimo Albergotti (1619-1669) fu decano del suo Collegio, prestò la sua opera in Firenze ed in Roma e godé delle amicizie legate alla corte medicea. Alla morte di Cosimo, il suo patrimonio fu presumibilmente conteso fra il Sen. Roberto Pandolfini, erede per testamento ed il fratello Albizo, già proprietario della restante metà del complesso di Gragnone.
Stà di fatto che bisognerà attendere il 31 luglio 1745, per ritrovare nei catasti la sequente nota: "...Un tenimento di più pezzi di terra lavorativa, vignata, parte querciata e castagnata, sodo con parte arborata e olivata, diviso per via che và a Roselleto, con casa da Padrone e Chiesa di staiora 54 posto nel Comune di Bossi luogo detto Col di Gragnone e Sala confina: I) fiume di Col di Gragnone, II) via che divide il Comune di Bossi con quello di Pieve al Bagnoro, III) fossato che divide detti comuni e altri beni del medesimo Cosimo Albergotti e cav. Albizo e via che va al Roselleto.
Stima 320;.....(elenco di altri beni)... si cassa il nome di Cosimo Albergotti già defunto e la presente posta incominciante in questo a carta 425 (Catasto antico Arezzo-Porta S.Spirito) si rinnova tutto in conto e faccia del colonnello Ferdinando del Sen. Camillo del Sen. Ruberto Pandolfini, erede mediante la persona del detto senatore Ruberto suo nonno di detto Cosimo Albergotti e da esso nella persona di detto Sen. Camillo suo padre entrambi defunti ed oggi detto colonnello Ferdinado, come figlio, nipote ed erede rispettivamente di detti suoi autori tutto con presenza ed istanza di Giovan Domenico Bonci agente del medesimo...".

Ministero per i Beni Culturali e Ambientali

SOPRINTENDENZA PER I BENI A.A.A.S. DI AREZZO

Priva della maggior parte degli ambienti padronali, l'attuale villa Albergotti passa nel 1672-1673 ai fratelli Alberico e Giovan Battista di Albizo, interessante a questo punto è la descrizione dei catasti "...Un tenimento di terre lavorative, vitate, arborate, olivate e vignate con alcuni quercioli con casa da padrone e lavoratore di stajora 13 nel detto comune di Bossi, luogo detto Col di Gragnone fino a tutta la Grillandetta o Rio della Doccia, a levante e ponente: case di Cosimo Albergotti, tramontana: via della Casella o Roselleto; ponente: loro detti e detto Cosimo Albergotti; mezzogiorno: fossato della Doccia e beni di detto Cosimo stimato fiorini 52". (Catasto Antico Arezzo-Porta S.Lorentino ac. I23v).

Notiamo che il complesso si riduce da 54 a 13 stajora, è privo di Chiesa e confina ancora, dopo quattro anni dalla morte, con Cosimo Albergotti ed ha una stima decisamente modesta.

La seconda metà del XVIII Sec. segna l'apogeo politico-economico della famiglia Albergotti, l'immobile di proprietà di Angelo Tommaso fu oggetto di notevoli ampliamenti per trasformarlo in villa-palazzo, gloria e vanto del casato, arricchito ora dall'acquisto del titolo di Marchese di Polino dalla antica famiglia Castelli.

Un ruolo di primo piano nella ristrutturazione della villa ebbe anche Monsignor Agostino Albergotti, fratello del neo-marchese Angelo Tommaso. Nato nel 1755, Agostino fu nominato nel 1802, dopo vari incarichi, vescovo di Arezzo. Si dedicò a riformare i Seminari fondò diverse case religiose, restaurò chiese ed edifici sacri della Diocesi e si distinse nel portare a termine la Cappella della Madonna del Conforto nella Cattedrale aretina, nonchè la Chiesa di S. Caterina, attigua a palazzo Albergotti e donata alla omonima Compagnia.

A Monsignor Agostino, che amava rifugiarsi nella sua villa di Gragnone, si deve la costruzione della Cappella, dedicata all'Immacolata Concezione, fra la fine del XVIII° Sec. e gli inizi del XIX° Secolo.

I lavori di ampliamento della villa proseguirono almeno fino al primo decennio dell'Ottocento, allorchè il complesso fu ereditato dal Marchese Giuseppe del fu Angelo Tommaso.

La descrizione dei catasti segnalano ora "...un palazzo ad uso di villa di n° 43 stanze da cima a fondo, con orto e i suoi annessi con Oratorio modernamente costruito cui confina: I° Sig.ra Contessa Cassandra Pandolfini con Villa; 2° e 3° beni infrascritti annessi a detta villa; 4° strada. Stmato: fiorini 190 che non si tirano fuori poichè atteso servire proprio uso.." (Volture 1807-Tomo II ac. 748).

Ministero per i Beni Culturali e Ambientali
SOPRINTENDENZA PER I BENI A.A.A.S. DI AREZZO

Costituita da più corpi di fabbrica, villa Albergotti presenta con un articolato gioco di volumi, un prospetto caratterizzato da finestre rettangolari disposte in asse e centrato da un portale bugnato che si collega al parco tramite un ponte in pietra.
Inglobata nella villa è anche la possente torre dell'antico mastio, svettante sull'intero complesso e affiancata da una aerea altana con arcate a sesto ribassato.

Cappella

Addossata alla villa c'è la cappella, racchiusa fra due lesene angolari con portale e soprastante finestra riquadrati in pietra.
L'interno, costituito da un'unica aula rettangolare è caratterizzato da decorazioni ad affresco trompe-l'oil del XIX° Sec. che oranano i portali, le nicchie, i confessionali, la cantoria e le finestre. L'altare in finto marmo, presenta anch'esso una trabeazione dipinta a trompe-l'oil incorniciante una tela del XVII-XVIII° Sec. raffigurante l'Immacolata Concezione.
Degni di nota il cassettonato del soffitto, la balaustra lignea che delimita la zona transettoriale, le due acquasantiere in marmo ed infine le quattro tele barocche raffiguranti Santi poste nelle nicchie soprastanti le aperture laterali.

Primo terreno

Adibito a locali di fattoria, il piano terreno della villa, presenta numerose testimonianze del fortilizio medioevale, portali, finestre tamponate e stemmi a "ferro di vanga" del XIII-XVI° Sec., si alternano ad elementi più recenti quali per esempio i soffitti a travatura lignea in sostituzione delle antiche volte di cui resta qualche traccia nelle possenti murature in pietra a filaretto. Dal piano terreno, una scalinata in pietra con capi rampa finemente decorati con l'arme Albergotti guadagna i piani superiori.

Primo piano

Arricchito da ampie sale di rappresentanza, il primo piano è frutto degli ammodernamenti operati dai fratelli Angelo Tommaso e Agostino Albergotti. In gran parte pavimentati in cotto, le sale, con riquadri e decorazioni ottocenteschi, presentano caminetti del XVIII-XIX° Sec. in pietra o finto marmo. Da sottolineare la cucina con l'acquaio del XVII° Sec. ed il camino coevo, entrambi in pietra, nonchè il salone principale, dominato dai ritratti degli antenati di casa Albergotti oltre che dal monumentale camino rinascimentale, finemente decorato con frontale centrato dall'arme della famiglia.

MODULARIO B.C. - 3

Ministero per i Beni Culturali e Ambientali

SOPRINTENDENZA PER I BENI A.A.A.S. DI AREZZO

Adibito a zona notte, il secondo piano è caratterizzato invece da alcova e boudoirs oltre che da ambienti per la servitù.
Completano la villa, le soffitte e l'altana, quest'ultima con splendida vista sul parco. Punteggiato da secolari siepi di bosso che delimitano il pomaio, il giardino all'italiana, la limonaia, le serre e la passeggiata, il parco, d'impianto tardo settecentesco è arricchito dalla presenza di pini e cipressi che circondano il complesso esaltandone la bellezza e schermandone la privacy.
Tramite un piccolo viale che prosegue fino alla Strada Provinciale per Calbi, Villa Albergotti si collega alla attigua Villa Pandolfini.
Quest'ultima, articolata su tre piani è caratterizzata da tre serie di aperture assiali, centrate da un portale bugnato sottolineato da una scalinata posticcia.
Il Seicentesco prospetto, arricchito al piano terreno da una serie di sei finestre inginocchiate, è affiancato dal coevo Oratorio di S.Cristina, oltre che da un arborato giardino antistante la Strada Provinciale e lungo il torrente Vingone.
Racchiusa fra due lesene angolari con soprastante timpano triangolare, la cappella è caratterizzata, in facciata, da una finestrella barocca con sottostante portale rettangolare.
Purtroppo l'impossibilità di visitare la villa, non ci permette, attualmente, una descrizione degli ambienti interni.
Per quanto sopra esposto dato l'intrinseco valore storico-architettonico delle ville Albergotti-Pandolfini, si ritiene necessario vincolare esternamente ed internamente il suddetto complesso ai sensi degli artt. 1 e 3 della legge 1.6.1939, n° 1089.

IL RELATORE
Geom. Pietro Frappi

L'ARCHITETTO DIRETTORE COORDINATORE
(Arch. Carla Corsi)

IL SOPRINTENDENTE
PRIMO DIRIGENTE
(Dott.ssa Anna Maria Maetzke)

VISTO:
IL DIRETTORE GENERALE
Dott. Mario Serio

A.3

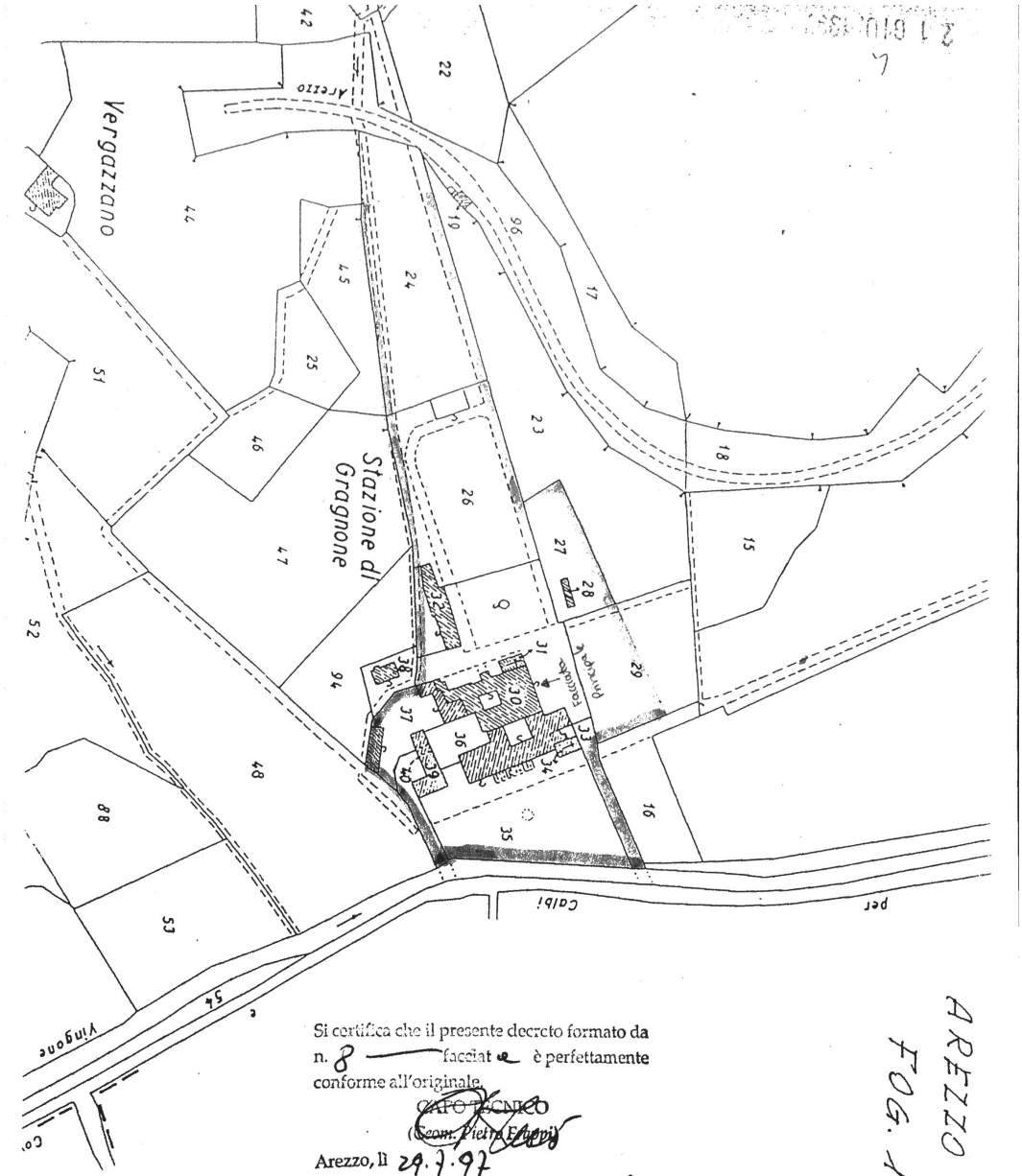
Versazzano
Stazione di Gragnone
Arezzo
Si certifica che il presente decreto formato da
n. 8 facciat e è perfettamente
conforme all'originale.
CAPO TECNICO
(Geom. Pietro Fabbri)
Arezzo, li 29.7.97
AREZZO A
FOG. 192
152

A.4

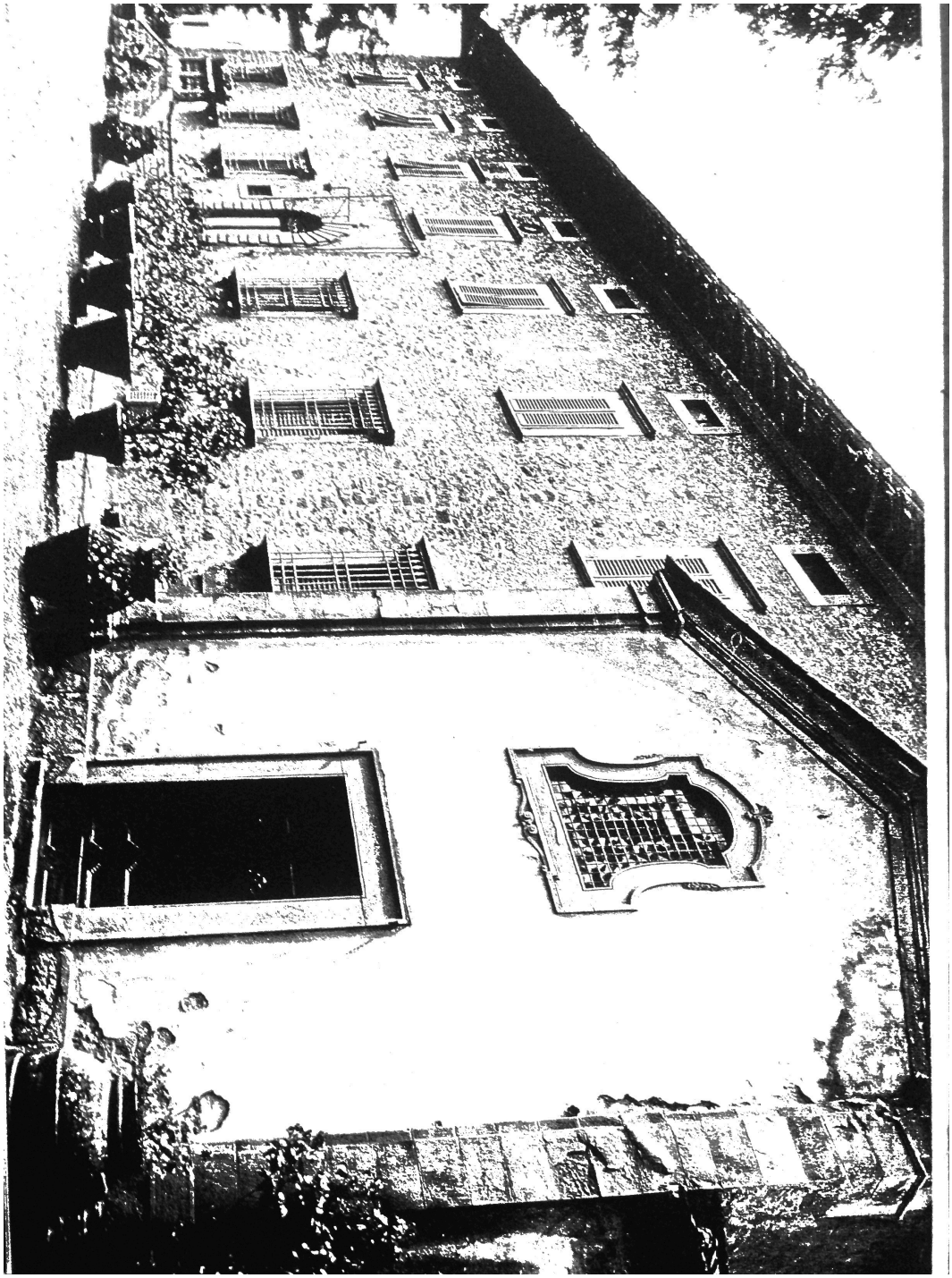

A.5

Index of pictures

Picture 1. Building location....14
Picture 2. Aerial view....14
Picture 3. Aerial view 2....15
Picture 4. Main facade....16
Picture 5. Two orders timber beam slab 1....17
Picture 6. Two orders timber beam slab 2....18
Picture 7. Two orders timber beam slab 3....18
Picture 8. Example of little vaults 1....19
Picture 9. Example of little vaults 2....19
Picture 10. First floor roof connections....20
Picture 11. Second floor roof connections....20
Picture 12. Inner connections of first floor roof....21
Picture 13. Detail of an Inner connection of first floor roof....21
Picture 14. Particular 2 of an Inner connection of first floor roof....22
Picture 15. Plan view reconstruction....24
Picture 16. Ground floor plan view....25
Picture 17. Raised ground floor plan view....25
Picture 18. First floor plan view....26
Picture 19. Use of photograph to orientate and define the façade reconstruction....27
Picture 20. Main façade reconstruction....28
Picture 21. Lateral façade reconstruction....28
Picture 22. Final front façade....29
Picture 23. Different kind of transversal sections....33
Picture 24. Example of mixed masonry....36
Picture 25. Example of ordinary masonry....37
Picture 26. Schematization of a SDOF system....40
Picture 27. Scheme of a MDOF system....41
Picture 28. Capacity curves of a real system....42
Picture 29. Bilinear (left) and trilinear (right) linearization of the capacity curve of a real system....43
Picture 30. Schematization of hardening (i), perfect (p) and softening (d) trend....44
Picture 31. Representation of a bilinear capacity curve....44
Picture 32. Capacity Spectrum Method....46
Picture 33. Relationship between spectral acceleration and spectral displacement....47
Picture 34. Inelastic response spectra for constant ductility in S_D-S_A plane....50
Picture 35. General scheme for the evaluation of the equivalent bilinear curve....52
Picture 36. Elastic and inelastic spectra and bilinear capacity curve....53
Picture 37. Limit lines and tangent circle according to Mohr-Coulomb....55
Picture 38. Gravity option window....61

Picture 39. Ground floor slab disposition....63
Picture 40. Raised ground floor slab disposition....63
Picture 41. First floor slab disposition....64
Picture 42. Front wall capacity curve....68
Picture 43. Right handside wall capacity curve....68
Picture 44. Left handside wall capacity curve....69
Picture 45. Back wall capacity curve....69
Picture 46. Front wall: MDOF and SDOF bilinear capacity curves....70
Picture 47. Right handside wall: MDOF and SDOF bilinear capacity curves....71
Picture 48. Left handside wall: MDOF and SDOF bilinear capacity curves....71
Picture 49. Back wall: MDOF and SDOF bilinear capacity curves....72
Picture 50. Front wall YY stress and deformed shape....73
Picture 51. Right handside wall YY stress and deformed shape....73
Picture 52. Left handside wall YY stress and deformed shape....74
Picture 53. Back wall YY stress and deformed shape....74
Picture 54. Elastic design spectra....77
Picture 55. Inelastic design spectrum (SLV)....78
Picture 56. Front wall acceleration-displacement capacity curve....78
Picture 57. ADSR inelastic design spectrum (SLV)....79
Picture 58. Right handside wall acceleration-displacement capacity curve....79
Picture 59. Left handside wall acceleration-displacement capacity curve....80
Picture 60. Back wall acceleration-displacement capacity curve....80
Picture 61. Superposition for SLV – Front wall....82
Picture 62. Reduction of inelastic spectrum for SLV – Front wall....82
Picture 63. Reduction of inelastic spectrum for SLV – Right handside wall....84
Picture 64. Reduction of inelastic spectrum for SLV – Left handside wall....84
Picture 65. Reduction of inelastic spectrum for SLV – Back wall....85
Picture 66. Superposition for SLD – Front wall....86
Picture 67. Superposition for SLD – Right handside wall....86
Picture 68. Superposition for SLD – Left handside wall....87
Picture 69. Superposition for SLD – Back wall....87
Picture 70. Timber-brick slab....90
Picture 71. Reinforced timber beam....91
Picture 72. A reinforced timber slab....92
Picture 73. Consequence of excessive rigidity of the cloak....94
Picture 74. Example of strengthening work....95
Picture 75. Example of tie-rod disposition....95

Index of tables

Table 1. Concrete properties....60
Table 2. Self weight for each wall....62
Table 3. Slab Load result....64
Table 4. Vertical load over the slabs....65
Table 5. Main results of the modal analysis....66
Table 6. Design horizontal forces....67
Table 7. Initial parameters setting....75
Table 8. Parameters for SLV....77
Table 9. Parameters for SLD....77
Table 10. Displacement verification SLV....83
Table 11. Displacement verification SLD....86

BLUEPRINTS